Percolation-Based Metrics to Quantify Resilience and Performance of Communication Systems

by Caesar S. Benipayo

B.S. in Electronics and Communications Engineering, March 1979, University of Santo Tomas
Master's in Engineering Management, May 2000, Old Dominion University
Master's in Business Administration, May 2012, Georgetown University

A Praxis submitted to

The Faculty of
The School of Engineering and Applied Science
of The George Washington University
in partial fulfillment of the requirements
for the degree of Doctor of Engineering

January 10, 2019

Praxis directed by

Amir Etemadi
Assistant Professor of Engineering and Applied Science

Ebrahim Malalla
Visiting Associate Professor of Engineering and Applied Science

The School of Engineering and Applied Science of The George Washington University certifies that Caesar Sanosa Benipayo has passed the Final Examination for the degree of Doctor of Engineering as of October 17, 2018. This is the final and approved form of the Praxis.

Percolation-Based Metrics to Quantify Resilience and Performance of Communication Systems

Caesar S. Benipayo

Praxis Research Committee:

Amir Etemadi, Assistant Professor of Engineering and Applied Science, Praxis Co-Director

Ebrahim Malalla, Visiting Associate Professor of Engineering and Applied Science, Praxis Co-Director

Timothy Blackburn, Professorial Lecturer of Engineering Management and Systems Engineering, Committee Member

[1] Portions of information contained in this publication/book are printed with permission of Minitab Inc. All such material remains the exclusive property and copyright of Minitab Inc. All rights reserved.

Dedication

The author would like to dedicate this praxis to his wife, Jacqueline Campbell Benipayo, his friend and companion who have faith in him and supported this effort in every way possible.

The author would also like to dedicate this Doctorate milestone to his children Nicholas Campbell Benipayo and Natasha Benipayo Kerem for their patience, love, and outstanding moral support. He hopes that his dedication to continuous education will serve as a model to them as they commence their professional careers.

Finally, to the author's mother, Marina Benipayo, for showing him that education is a life-long journey.

Acknowledgments

The author wishes to acknowledge Dr. Michael Green and Dr. Blake Roberts for their mentorship and guidance during his tenure as a Ph.D. student. They have provided flexibility and time to review his journal articles. He would not have completed this milestone without their kind support during the past two years.

He would like to acknowledge the social network analysis software, Gephi, for the use of the open source software. This software tremendously helped in converting the raw data to determine the network centralities and computations. The author would like to give special recognition to Professor Albert-Laszlo Barabasi of the Center for Complex Network Research for providing the western power grid dataset and the introduction of network science concepts. The electrical power grid datasets allowed the author to validate the model. Lastly, to Captain Brian Metcalf and NAVSEA PMS 317 Staff, for their support and confidence in his research allowing the author to use the functional interface requirement document data sets and collaborate with subject matter experts.

He would like to acknowledge a special recognition to ICI Services Corporation for their financial support and work flexibility during his research studies.

Finally, the author would like to acknowledge Dr. Amir Etemadi, Dr. Ebrahim Malalla and Dr. Timothy Blackburn for their insight on his Praxis and getting to the finish line.

Abstract of Praxis

Percolation-Based Metrics to Quantify Resilience and Performance of Communication Systems

Resilience theory plays a vital role in the practical design of modern engineered resilient systems composed of cyber-physical systems and components having interdependencies intended to make the entire system robust. In this paper, the percolation-based metric is applied to measure the communication systems' resilience and efficiency. Because there is no consistent and reliable way to measure resilience, the percolation-based metric framework is developed to model the component or system failure by removing fractions of the nodes or links, causing the network to transition from functional to non-functional. The utility of the percolation-based metric model is demonstrated by using the power grid and maritime platform systems (legacy and future design versions) as case studies. The results from analyses of the maritime communication and power grid systems are presented. The results indicate that percolation-base metric may be a useful approach for system engineers and designers to gain improved insight into the quantification of communication system resilience and efficiency.

Table of Contents

List of Figures

List of Tables

List of Acronyms

BN	Bayesian Network
BBN	Bayesian Belief Network
CDF	Cumulative Distribution Function
CIM	Component Importance Measure
CPS	Cyber-Physical System
DAU	Defense Acquisition University
DHS	Department of Homeland Security
DOD	Department of Defense
ETA	Event Tree Analysis
EU COST	European Union Cooperation in Science Technology
FFIP	Functional Failure Identification and Propagation
FFR	Functional Failure Reasoning
FIRD	Functional Interface Requirements Document
FMEA	Failure Mode Effects Analysis
FMECA	Failure Mode Effects Criticality Analysis
FTA	Fault Tree Analysis
MA	Markov Analysis
MC	Markov Chain

MOP	Measure of Performance
MOE	Measure of Effectiveness
NAVSEA	Naval Sea System Command
NIST	National Institute of Science and Technology
PDF	Probability Density Function
PHM	Prognostic and Health Management
PRA	Probabilistic Risk Assessment
QOS	Quality of Service
RBDO	Reliability-Based Design Optimization
RDSD	Resilience-Driven System Design
SE	System Engineering
WAN	Wide Area Network
WWW	World Wide Web

Glossary of Terms

Betweenness centrality: "a measure of the number of paths that traverse each edge" (Estrada, 2012).

Closeness centrality: a measure of the nearness of an object to the other objects in the network (Estrada, 2012).

Complex system: a system made of linked parts which display emergent properties that are not evident from the characteristics of the individual parts (Estrada, 2003).

Cyber-Physical System: the integration and collective effort between the communication and physical assets to generate and provide a constant source of merchandise and services (Rinaldi, 2001).

Cyber System: any grouping of infrastructures with services, equipment, workforce, and telecommunication network that is aggregated to provide cyber amenities (NIPP, 2009).

Clustering coefficient: an index that measures the "ratio of three times the number of triangles divided by the number of connected triples." It is used to measure robustness such as high clustering coefficient shows high robustness due to the number of other paths increases with the number of triangles (Ellens, 2013; Estrada, 2003).

Critical infrastructure: the facilities and resources crucial to the country in which the failure of or damage to such infrastructures and resources have a harmful effect on the economy, safety, public health, and security (NIPP, 2013).

Degree centrality: a measure of an object's connection by totaling the number of direct links each object has to others in the network (Estrada, 2012).

Eigenvector centrality: a measure of an object's connections and the direct influence it has over other connected objects in the network (Estrada, 2012).

Emergent behavior: a coherent system-wide property that cannot be inferred directly by analyzing the behavior of individual components (Dabrowski, 2006).

Graph Theory: a study of networks in statistical mechanics that represent the inter-connections of a system consisting of nodes (N) and links (L), with the node representing the system elements while the links characterize interconnection among nodes (Estrada, 2012).

Interdependence: a representation of the physical, cyber, geographic, or logical relationship between two infrastructures wherein the status of one structure influences the other structure's status (Rinaldi, 2001; Buldyrev, 2010; Raghav, 2012; Huang Z. 2015).

Maintainability: a design attribute that can be expressed regarding maintenance frequency factors, elapsed time, and cost (Blanchard, 2003).

Measure of effectiveness (MOE): the data used to measure the mission accomplishment that comes from using the system in its expected environment (DAU, 2018).

Measure of performance (MOP): performance-related factors that are identified to satisfy the requirements such as time, velocity, size, or other distinctly measurable performance features (Blanchard, 2003).

Network (graph): a group of elements that communicate information or act together to perform a function (NIPP, 2009).

PageRank centrality: a variation of the Eigenvector centrality measure for the directed network (Estrada, 2012).

Rapidity: the ability of the system to meet significant functions and accomplish restoration goals promptly to mitigate losses and further disruptions (Bruneau, 2003).

Redundancy: the degree to which network components are replaceable and able to function after a disruptive event, degraded function, or component failure (Bruneau, 2003).

Reliability: "the probability that s system will perform its designed function for a stated time under a set of environments" (Youn, 2011; Lewis, 1994).

Resilience: the system's ability to withstand a disruptive event by reducing the initial shock, adjusting its function, and recovery (Nan, 2016).

Resourcefulness: measures the organizational capability to recognize problems, set urgencies, and organize resources during the incidence of a disastrous event (Bruneau, 2003).

Restoration: the system's ability to bring back its original capacity and performance when disruptions occur (Youn, 2011).

Robustness: the capacity of the structure to endure a disturbance without degradation in performance or a loss of function (Bruneau, 2003; Rosas-Casals, 2007; Ellens, 2013).

Sector: a group of resources, organizations, or networks that deliver a standard purpose for the financial system, administration, or the public (NIPP, 2009).

Vulnerability: a “physical or operational” characteristic that causes an object susceptible to manipulation or prone to a possible threat. (DHS, 2010).

Chapter 1: Introduction

1.1 Background

Over the years, there have been significant studies on the effects of disruptive events on resiliency and efficiency of communication systems (Rad, 2014; Dikbiyik, 2014; Martins, 2017). The disruptive events are generally triggered by "natural disasters, technology-driven failures, or adversarial attacks" which have significant financial and social impacts (Small, 2017; Mauthe, 2016). These disaster-based breakdowns are more stochastic and wide-ranging in scale compared to random breakdown which usually leads to immediate failure of network communication systems located in various geographical areas (Rak, 2016). Therefore, there is a need to minimize the impact of disaster-based failures through the deployment of resilient and efficient communication systems.

The United States has 16 critical infrastructure sectors[2] such as the defense industrial base, information technology, energy, transportation, and others; which are heavily dependent on communication systems (DHS, 2017). For instance, the latest hurricane (Michael) that hit Panama City, Florida devastated the telecommunication and power grid systems which impacted the emergency services lines of communication throughout the storm (Sullivan, 2018). Another example is the catastrophic damage caused by hurricane Maria to the island of the Dominican Republic with island-wide communication black-out. These examples show the interdependencies between the communication system and

[2] There are 16 critical infrastructures sectors namely: "Chemical, Commercial Facilities, Communications, Critical Manufacturing, Dams, Defense Industrial Base, Emergency Services, Energy, Financial Services, Food and Agriculture, Government Facilities, Healthcare and Public Health, Information Technology, Nuclear Reactors, Materials and Waste, Transportation and Water and Wastewater systems."

the power grid. The power grid SCADA[3] depends on the communication system to provide control signals, and the communication system relies on the electrical grid to provide its power supply (Parandehgheibi, 2013; Chen, 2018).

Today, resilience theory is approached from different viewpoints and is defined differently across various domains to include "organizational, social, economic, and engineering domains" (Hosseini, 2016). For instance, Hosseini et al. define resilience as "*the ability of a system to return to normal conditions after the occurrence of a disruptive event.*" The Department of Homeland Security defines resilience as *"the ability to prepare for and adapt to changing conditions and withstand and recover rapidly from disruptions such as deliberate attacks, accidents, or naturally occurring threats or incidents."* The European Cooperation in Science and Technology (EU COST) defines communication network resilience as *"the network's ability to maintain the same level of functionality in the face of internal changes and external disturbances as a result of large-scale natural disasters and corresponding failures, weather-based disruptions, technology-related disasters, and malicious human activities"* (Mauthe, 2016; EUCOST, 2018). Bruneau et al. defined four system attributes of seismic resilience as *robustness*[4], *rapidity*[5], *resourcefulness*[6], *and redundancy*[7] (Brunuea, 2003). Since there is no

[3] SCADA is an acronym for "supervisory control and data acquisition". It is a computer system application that is used to monitor and control power plant equipment.
[4] Robustness: "is the strength of system or its ability to prevent damage propagation through the system in the presence of a disruptive event."
[5] Rapidity: "is the speed or rate at which a system could return to its original state or at least an acceptable level of functionality after the occurrence of a disruption."
[6] Resourcefulness: "it is the level of capability in applying material (i.e., information, technology, physical) and human resources (i.e., labor) to respond to a disruptive event."
[7] Redundancy: "the extent to which carries by a system to minimize the likelihood and impact of disruption."

consistent approach to measuring system resilience, in this praxis the focus will be on system robustness based on previous work by Cohen and Sole (Cohen, 2000; Sole, 2007).

Designing a resilient communication system requires the development of percolation-based metrics that can quantify resilience (robustness) and efficiency to allow designers to compare different system architectures and make informed decisions. In this praxis, the maritime platform communication systems (legacy[8] and future[9] versions) and power grid systems were used as case studies to show the utility of the percolation-based metrics. The maritime platform is used in the case study because of their critical role in defending the United States. These platforms are usually required to withstand disruptive events, rapidly recover, and continue to function in their operational environment. Georger et al. describe the maritime platform as systems that are *"expected to be trusted and effective in a wide range of operational environment with the ability to respond to new requirements through new tactics, appropriate reconfiguration, and timely replacement"* (Georger, 2014). Since there is no published resilience and efficiency metrics for the maritime platform, the published datasets for the Italian power grid (ENTSOE, 2017; Sole et al., 2007 Table 1) and the Western power grid (Watts, 1998) were used for model validation and use as a baseline for comparison with the maritime platform communication system's resilience and efficiency. In this praxis, only the Italian power grid is used for comparison because it has the published robustness and efficiency data. The published data for the Italian and Western power grids are shown in Chapter 5 Table 5-1.

[8] Legacy maritime platform: denotes for the original design of the maritime platform built in the early 1990s.
[9] Future maritime platform: denotes for the new design of the maritime platform that is currently under construction.

1.2 Problem Statement

Currently, there is no metric in the literature to quantify resilience (robustness) and efficiency of communications systems. Using the Web of Science (WOS) database to search for studies in "resilience" resulted in a total of 101 domains, of which the largest about resilience was that of the psychological followed by the environmental, social, and ecological domains (see Figure 1-1 and Appendix A). However, only a tiny percentage of the study is in the engineering domain. Furthermore, a literature search for "resilience and percolation" produced only 25 papers, with four publications dedicated to the application of percolation in networks. This deficiency provides an opportunity to impact resilience research in the engineering domain, and this praxis is concerned with using quantitative methodologies as a tool to measure communication system resilience and performance (efficiency). Therefore, the details and scope of other resilience measurement techniques are omitted because these methods could not be given the proper attention here.

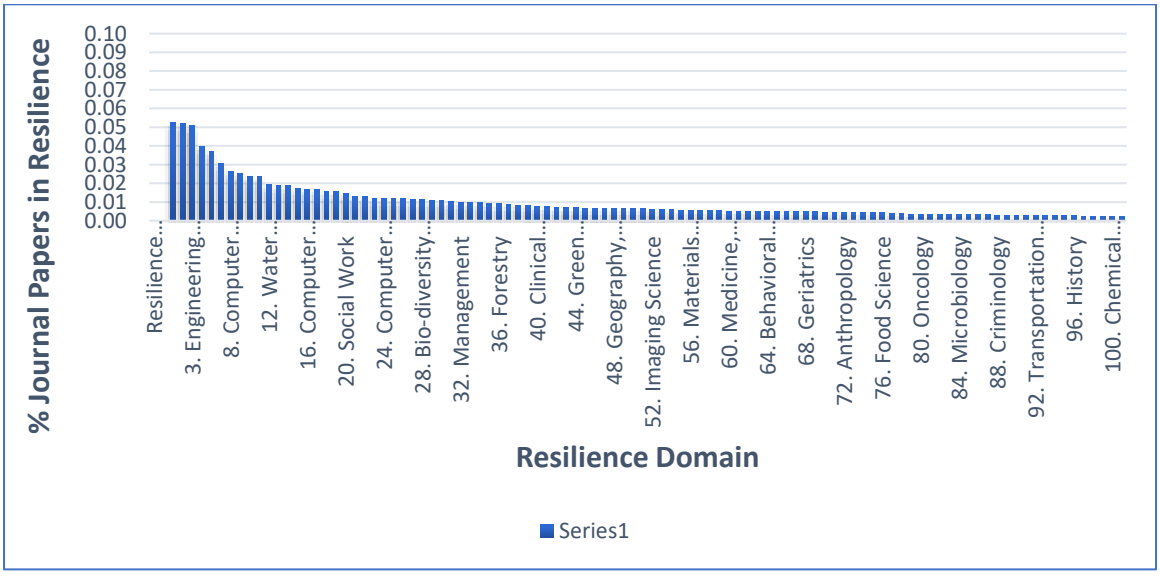

Figure 1-1: Resilience journal population

Resilience is a system level attribute closely associated with survivability, reliability, robustness, elasticity, safety, and nimbleness (Uday, 2015: Song, 2016). Although many scholars have conducted extensive studies on resilience design (Callaway, 2000; Youn, 2011; Filippini, 2012; Jackson, 2013; Francis, 2014; Bhatia, 2015; and Bahun, 2016; and others), only a few papers applied resilience to maritime systems (Song, 2016). A significant knowledge gap exists in current understandings of maritime system interdependencies and the communication system's performance during a disruptive event. Thus, a quantitative method for analyzing the maritime communication system's resilience and efficiency has yet to be defined.

1.3 Thesis Statement

Percolation and social network theory can be used to quantify communication system's resilience and efficiency.

Background: The technological breakthrough in computing and data storage at the turn of the 21st century has revolutionized the rise of network science, resulting in the mapping of complex, interdependent, and resilient systems such as the World Wide Web, the Internet, the protein to protein interactions in human cells, and social networks such as Linkedin or Facebook, as well as tracing neural connections in the mammalian brain (Barabasi, 2016). A visual mapping tool that can illustrate a complex system like a wiring schematic diagram is needed to define the behavior or response of a system that contains hundreds to billions of interacting components. One of the many visualization and mapping techniques employed in network science is the social network analysis (SNA) tool. This tool helps the analyst understand the interaction among data and identify the critical nodes within the graph. Examples of top SNA tools include

Centrifuge, Commetrix, Cuttlefish, Cytoscape, Egonet, Gephi[10], and others (Desale, 2018).

Figure 1-2 presents a sample output of the Gephi software describing the Legacy maritime platform. The first row shows the centrality measures[11] such as "degree centrality, closeness centrality, betweenness centrality, PageRank centrality, and eigenvector centrality" (Estrada, 2012). Due to the vast number of dependencies among the various systems, using the SNA to present the entire maritime platform's topology and the concentration of important hubs that impact the system's resilience and efficiency is practical. In this praxis, we use robustness as a proxy for resilience. Figure 1-3 presents the legacy maritime platform communication systems' interconnections. Figure 1-4 shows the legacy maritime platform's topology showing the concentration of nodes called hubs or clusters and the overall network topology.

[10] Gephi software: an open-source software package for network analysis and visualization. It is authored in "Java on the NetBeans" platform that was created by a non-profit organization called Gephi Consortium.
[11] Centrality measures: "identifies the most important nodes in the network. Some of the most pertinent centrality measures are: degree centrality, closeness centrality, betweenness centrality, Eigen-vector centrality, and PageRank centrality."

id	label	timeset	qty	remarks	indegree	outdegree	degree	weighted	weighted	weighted	eccentrici	closenessc	harmonic	betweene	authority	hub	modularit	pageranks	componer	strongcon	clustering	eigencentrality
1	Surveillance Systems		1		0	10	10	0	10	10	6	0.244637	0.293739	0	0	9.18E-07	2	5.28E-04	0	463	0	0
2	SPS48		1		22	75	97	22	75	97	7	0.218	0.291044	29410.4	1.81E-06	4.28E-05	2	0.009719	0	462	1.54E-04	0.008103
3	SPQ9B		1		6	18	24	6	18	24	8	0.190227	0.217654	5202.2	5.02E-06	4.68E-06	2	0.001416	0	462	0	0.006283
4	SPS73		1		2	12	14	2	12	14	7	0.260766	0.28612	2672.436	3.63E-06	1.72E-04	2	6.53E-04	0	462	0.012821	0.002369
5	USG2A		1		8	12	20	8	12	20	7	0.244395	0.267902	3005.511	1.05E-04	7.55E-06	14	0.002717	0	462	0	0.057104
6	UPX29		1		17	23	40	17	23	40	6	0.210019	0.238379	8364.22	8.29E-07	2.37E-05	0	0.005044	0	462	0.001783	0.016386
7	UPX28		1	CHANGED	3	12	15	3	12	15	1	1	1	3792	6.83E-09	0	0	0.001514	0	143	0	9.17E-04
8	SLQ32B		1	CHANGED	11	23	34	11	23	34	9	0.158463	0.188082	11456.49	5.23E-06	2.42E-05	1	0.00396	0	462	0.007389	0.060268
9	ULQ16		1	CHANGED	4	3	7	4	3	7	10	0.145889	0.15653	1165.319	6.83E-09	1.96E-06	1	0.001402	0	462	0	0.001813
10	SLA10B		1		6	2	8	6	2	8	3	0.5	0.633333	485.2879	2.06E-06	1.87E-06	15	0.001368	0	5	0	0.004037
11	KAS1A		1		3	2	5	3	2	5	1	1	1	634	5.00E-08	0	2	0.001789	0	2	0	7.22E-04
12	Crypto Systems		1		0	3	3	0	3	3	9	0.173943	0.184496	0	0	3.12E-10	3	5.28E-04	0	465	0	0
13	SSEEF		1		1	1	2	1	1	2	8	0.209086	0.22292	747.4799	2.32E-12	3.64E-05	3	6.77E-04	0	464	0	1.98E-04
14	TACINTEL2		1		4	1	5	4	1	5	9	0.193116	0.204333	3047.055	2.09E-08	4.56E-06	3	0.001545	0	462	0	0.001254
15	SICOMM		1		4	1	5	4	1	5	1	1	1	315	2.09E-08	0	3	0.001901	0	29	0	0.001306
16	Shipboard Control Systems		1		0	4	4	0	4	4	8	0.178839	0.201465	0	0	6.30E-05	7	5.28E-04	0	466	0	0
17	ECS		1		11	37	48	11	37	48	9	0.196498	0.235351	11331.16	0.007036	4.57E-06	4	0.001583	0	462	0	0.05715
18	MSCS		1		8	2	10	8	2	10	8	0.190559	0.199674	114.9262	1.20E-04	3.74E-06	7	0.002152	0	462	0	0.039
19	SCS		1		18	6	24	18	6	24	7	0.206775	0.221968	1254.016	0.001275	1.68E-04	7	0.004557	0	462	0.007895	0.120771
20	ICAS		1		3	4	7	3	4	7	8	0.193067	0.205331	416.4621	3.34E-05	3.79E-05	7	0.00105	0	462	0	0.001581
21	Mission Control Systems		1		0	10	10	0	10	10	7	0.21311	0.254812	0	0	1.94E-05	5	5.28E-04	0	467	0	0
22	SPQ14		1		16	6	22	16	6	22	8	0.174121	0.19027	1456.983	5.96E-06	9.86E-06	15	0.006188	0	462	0.052632	0.019407
23	SSDS		1		39	14	53	39	14	53	7	0.224478	0.24653	16027.01	2.98E-04	0.001658	13	0.015674	0	462	0	0.185791
24	ACGKSQ		1		10	13	23	10	13	23	10	0.164263	0.182484	5030.172	3.97E-04	4.23E-06	5	0.003723	0	462	0.025974	0.017022
25	EPLRS		1	CHANGED	6	11	17	6	11	17	9	0.195892	0.216042	4110.522	3.35E-07	3.52E-05	5	0.003095	0	462	0	0.001834
26	GCCSM		1	CHANGED	37	50	87	37	50	87	9	0.205218	0.255092	21573.11	0.00153	1.10E-04	12	0.013483	0	462	0.001166	0.045273
27	NTCSS		1		10	6	16	10	6	16	10	0.150761	0.162984	3327.876	3.79E-04	1.13E-05	11	0.005448	0	462	0	0.008598
28	CDLMS		1		6	3	9	6	3	9	10	0.135092	0.141769	1979.88	4.12E-07	3.74E-06	11	0.003479	0	462	0	0.003716
29	TACAN		1		5	6	11	5	6	11	8	0.183855	0.19597	4862.9	9.06E-07	1.33E-05	15	0.003641	0	462	0	0.001737
30	SGSI		1		4	7	11	4	7	11	10	0.132534	0.143658	3948.965	1.45E-07	3.74E-06	5	0.003297	0	462	0	0.001489
31	WOCLS		1		2	5	7	2	5	7	8	0.177897	0.190841	5043.566	1.45E-07	2.73E-06	5	0.001373	0	462	0	5.05E-04
32	Weapon Systems		1		0	4	4	0	4	4	8	0.210526	0.233696	0	0	9.36E-09	6	5.28E-04	0	468	0	0
33	RAM		1		7	27	34	7	27	34	13	0.106253	0.138718	9758.868	7.12E-07	2.71E-05	6	0.003767	0	462	0	0.012728
34	GWS		1	ADDED	5	7	12	5	7	12	11	0.128755	0.140993	6447.984	4.43E-07	6.54E-06	12	0.003067	0	462	0	0.00208

Figure 1-2: Sample output of the Gephi social network analysis software

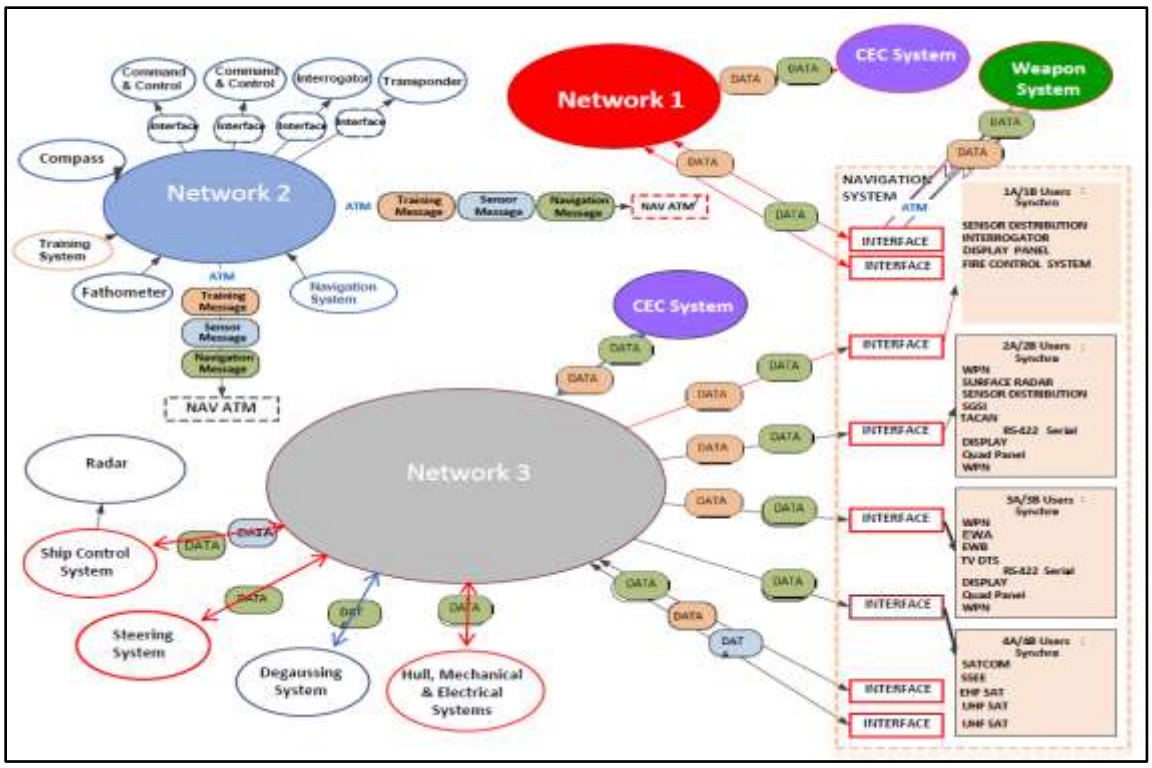

Figure 1-3: Example of maritime communication systems with interdependencies (Benipayo, 2016)

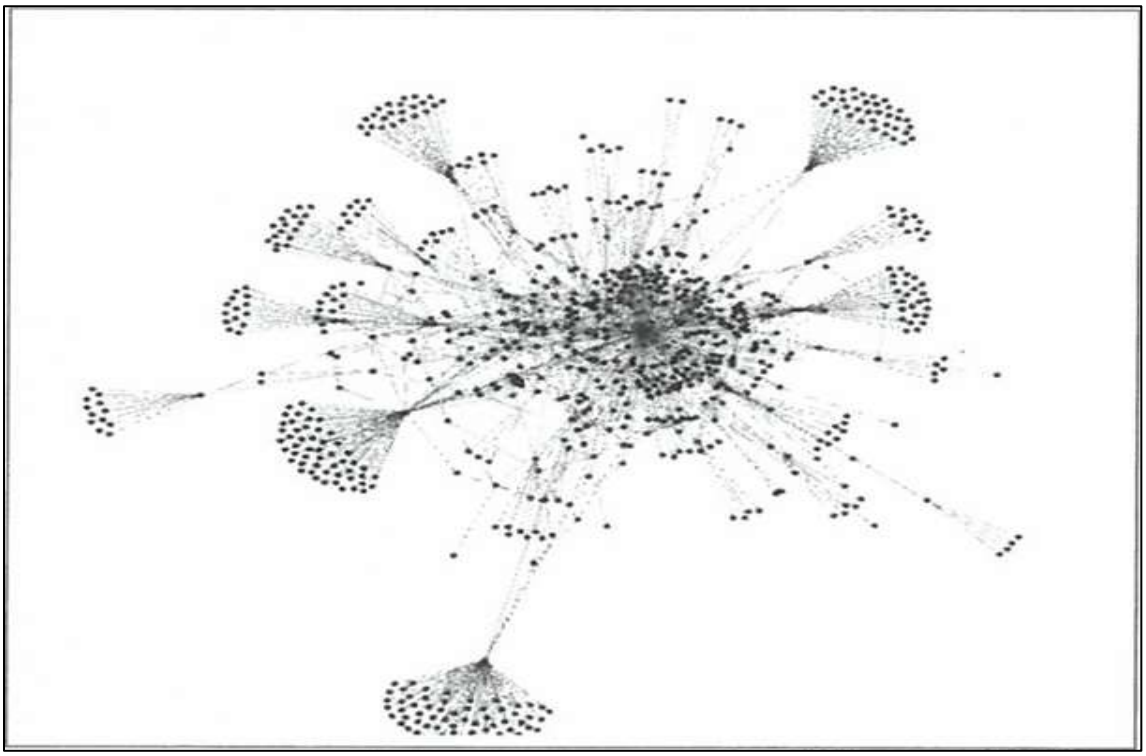

Figure 1-4: Example of Gephi visualization output

Percolation theory is applied to understand the impact of a disruptive event on the communication system's resilience (robustness) and efficiency. Percolation is a statistical mechanic's model that demonstrates a critical phenomenon called phase transition, meaning that there is a fundamental parameter in the model at which the behavior of the system drastically changes from nonfunctional to functional designated as percolation threshold (p_c). The phase transition from functional to nonfunctional is termed as the fragmentation threshold (f_c) [Barabasi, 2016 Chapter 8]. Section 3.2 provides a closer look into percolation threshold. Larger fragmentation threshold means that the system is robust because it will take a lot of nodes failing to breakdown the network.

The proposed percolation-based metric uses a maritime platform's functional interface requirements document (FIRD) to develop a network model that quantifies the communication system's normalized[12] robustness and efficiency. The system robustness and efficiency are determined by computing the fragmentation threshold (f_c) using equation (2-27) and efficiency ($E(G)$) using equation (3-3). The maritime platform communication system's robustness and efficiency are analyzed by examining the network failure using percolation theory. The percolation theory replicates the component failures or disruptive events by removing fractions of the nodes or edges resulting in the network transitioning from a functional network [1 means 100% connected] to a nonfunctional network [0 means 0% connection]. By applying percolation theory, systems that are complex, interdependent, and resilient can be analyzed, and system performance (efficiency) can be quantified.

[12] Normalized value: normalization allow the comparison of different datasets. The measured value is between 0 and 1.

1.4 Research Objectives

This praxis intends to develop a percolation-based metric framework that quantifies the communication system's resilience (robustness) and performance (efficiency). The framework should have simple computational and open source software requirements. The percolation-based metric framework should allow system designers to quantify resilience (robustness) and system performance (efficiency), compare communication systems under consideration and select the best system design that meets the system design requirements. The objectives of the praxis are the following:

1) Identify a quantitative metric(s) that can quantify resilience (robustness) and system performance (efficiency).
2) Use the power grid and maritime communication systems (legacy and future versions) as case studies to show the utility of the metrics developed.
3) Validate the quantitative model using published data from the power grid.
4) Identify a quantitative method that can measure components or systems interdependencies.

1.5 Research Questions and Hypotheses

This praxis discusses the development of a practical method of measuring the communication system's resilience and efficiency using an SNA tool and percolation theory. This method can generate a "rank-order-resilience" of system proposals that can inform engineering decisions. This praxis addresses the following questions:

RQ1: What quantitative metric(s) is best suited to measuring the maritime platform communication system's resilience (robustness) and system performance (efficiency)?

RQ2: How can we compare the resilience (robustness) and system performance (efficiency) of different maritime platforms to make better-informed decisions?

RQ3: Is there published data that can be used to validate the quantitative model?

The following hypotheses are tested to answer the research question #1:

Hypothesis 1. Percolation theory can be used to quantify resilience (robustness).

Hypothesis 2. Percolation theory can be used to quantify efficiency.

The following hypotheses are tested to answer the research question #2 and #3:

Hypothesis 3a. There is significant difference between the Legacy and Future communication systems resilience (robustness).

Hypothesis 3b. There is significant difference between the Legacy and Future communication systems efficiency.

Hypothesis 4a1. There is significant difference between the power grid and Legacy communication system resilience (robustness).

Hypothesis 4a2. There is significant difference between the power grid and Legacy communication system efficiency.

Hypothesis 4b1. There is significant difference between the power grid and Future communication system resilience (robustness).

Hypothesis 4b2. There is significant difference between the power grid and Future communication system efficiency.

1.6 Research Limitations

First, the difference in the fragmentation threshold (f_c) values between published and calculated Italian power grid data was due to the use of exponential degree distribution for the power grid, $P(k) = \frac{e^{\left(\frac{-k}{\gamma}\right)}}{\gamma}$, which results in a different formula, f_c = 1- ($\frac{1}{2\gamma-1}$), where γ is the average degree of the network, rather than the general fragmentation formula in Equation (2-27) (Sole, 2007 p.2; Rosas-Casals, 2007). Rosas-Casals et al. study has determined that the power grid has an exponential degree distribution, thus using the aformentioned formula. Secondly, there is no specific commercial software that computes the communication system's robustness (fragmentation threshold) and efficiency. Hence, the sample size of $n = 30$ was chosen due to the vast amount of time required to calculate the fragmentation threshold and efficiency for each individual node using an Excel spreadsheet. The author had to compute each nodal fragmentation threshold and efficiency (Italian power grid N = 329, legacy N = 782, and future N = 920), plot results, test hypotheses, and validate the data using the power grid data, which impacts the scheduled requirements to complete this research. For sample size $n \geq 30$, the sampling distribution of the means will approximate a normal distribution, and the test statistics are based on normal z-statistics (Spiegel, 1994 p.176). Finally, the FIRD access is limited, thus making it harder to compare with other DoD maritime platforms, and there is no known robustness (fragmentation threshold) and efficiency metric for the maritime platforms.

1.7 Organization of Praxis

The structured arrangement of this praxis provides a coherent approach that allows the readers to appreciate the researcher's rationale behind the study, methods, results of

research, analysis, and methods of arriving at conclusions. Specifically, the order for the praxis development is as follows:

Chapter 2: Literature Review. This section provides the theoretical foundation of this research through an in-depth review of functional failure analysis, quantitative resilience methods, traditional probability risk assessment methods, network science theory, and knowledge gap identification.

Chapter 3: Methods. This section provides the percolation-based metric framework; percolation threshold; dataset, collection, and preparation process; and method for computing communication system's robustness and efficiency.

Chapter 4: Results. This section presents the experimental results and hypotheses test developed in Chapter 3. Specifically, the data generated are based on a very specific case-study involving the power grid network and the legacy and future maritime platforms, and they are compared to address the problem statements.

Chapter 5: Discussion, Conclusion, and Future Research. This section discusses the experimental results and compares the communication system's robustness and efficiency. The conclusions support the problem statements. Future research and investigations are herein suggested.

Chapter 2: Literature Review

This chapter explains the focus of this research, that is, the search for resilience and efficiency performance metric that is suitable for measuring complex, interdependent, and resilient maritime platforms, as shown in Figure 2-1. In Section 2.1, the functional failure metric approaches across multi-disciplinary areas are reviewed. Next, the resilience theory and quantitative methods are discussed in Section 2.2. A review of the traditional reliability methods are covered in Section 2.3. The network theory covering social network analysis (SNA) and percolation theory is presented in Section 2.4. Finally, Section 2.5 discusses the gap in the body of knowledge relating to the resilience and performance metrics that we intend to address.

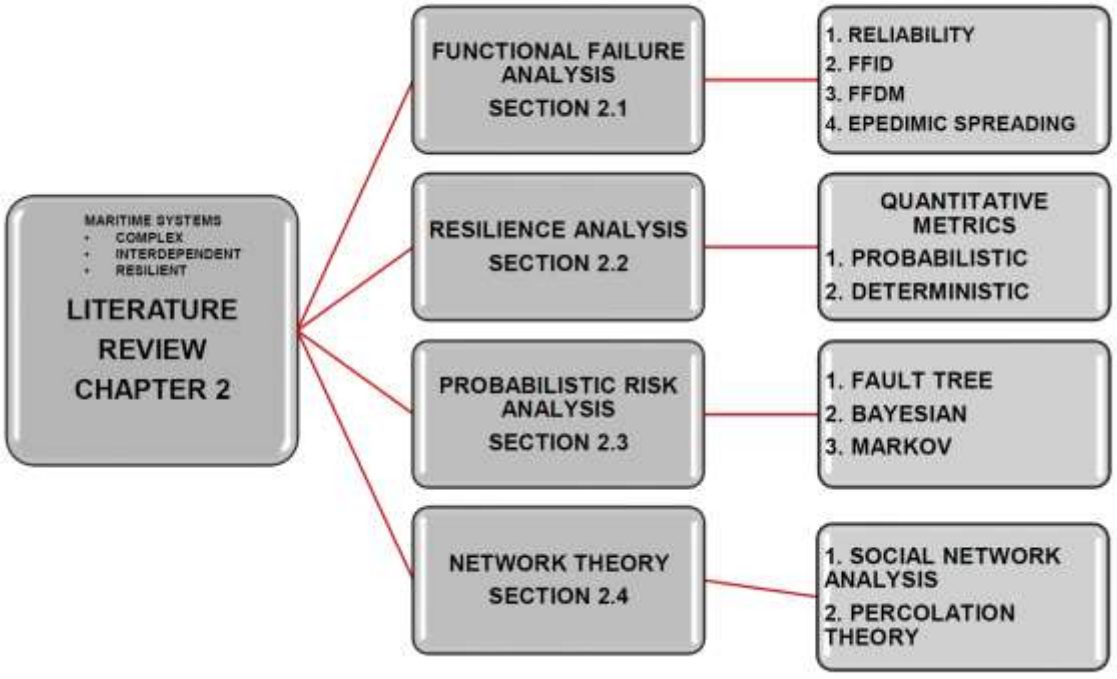

Figure 2-1: Literature research plan

2.1 Functional Failure Analysis

During the design processes, the broad outlines of the system functionality and product forms are articulated based on the stakeholder requirements definition and requirements analysis. The products of the design solution processes are "alternative design solutions, physical architectures, and ultimately a final design solution" (DAU, 2018). Some examples of the most common artifacts during the design processes are system illustrations, drawings, functional interface requirement documents, computer graphics, and basic concepts documenting the product development to meet operational requirements. This section discusses previous research on functional failure analysis.

Mehrpouyan et al. discuss the importance of developing a "reliability engineering tool" and "fault-tolerant tool" that can be applied throughout the design process of complex systems to manage the system's inherent uncertainty and its impact on life-cycle cost (Mehrpouyan, 2013; 2015). The authors use a disease-spreading model and a "non-linear dynamical system model" (Mehrpouyan, 2013) to analyze the army vehicle ramp system's failure propagation. Although graph theory was applied, the analysis was limited to a maximum node of only 70 nodes. Additionally, analyzing a system with multiple adjacency matrices would add more computations and time to create the adjacency matrices.

Uday and Marais's research expounds on the resilience assessment methodologies, resilience attributes, and challenges in designing resilient SoS (Uday, 2015). The authors also discuss the limitations of traditional reliability and risk assessment methods, such as FMEA/FMECA, FTA/ETA, BBN, and CIM, within the context of resilient SoS design.

Although this paper evaluates resilience design framework that includes principles, tools and models, and metrics, it does not specify how to quantify resilience and efficiency.

Kurtoglu and Tumer's research introduces a graph-based approach for analyzing system's functional failure risk instead of component failure analysis. The system top-level functional design is used to analyze system failures. An advantage of the "functional failure design method (FFDM)" (Kurtoglu, 2008 p.2) is the early discovery of probable failures by associating them with product functions. However, this method is unable to quantify the entire system's reliability to allow designers to compare various architectures.

Kurtoglu, Tumer, and Jensen's paper present a method of analyzing functional failures by using the "functional failure identification and propagation (FFIP) framework" (Kurtoglu, 2007 p.210). The authors use a "simulation-based failure analysis" (Kurtoglu, 2007 p.213) tool along with an "early-stage architecture framework" (Kurtoglu, 2007 p.209) that shows the impact of functional failures on architectural design. An advantage of this method is the identification of potential functional failures and their associated risks, saving potential resources later in the design process. A disadvantage of this model is that the user must be familiar with the process of developing functional models, functional dependency matrices, and propagation trees (Kurtoglu, 2010).

Ormon, Cassady, and Greenwood's paper presents simulation and analytical techniques to predict reliability and mean mission cost (Ormon, 2002). An advantage of this model is its simplicity, its use of known component failure rate, and its prediction of

component failure by using triangular probability method. However, this model does not account for system dependencies and reliance on component failure rate historical data.

2.2 Resilience Theory and Methods

Resilience theory plays a vital role in designing engineered systems comprised of CPSs with components, sub-systems, or system interdependencies intended to make the entire system robust. However, due to recent innovations in computational intelligence, automation, and control systems, the quantification of a system's resilience is associated with new technical challenges, one of which is the development of "reliable and consistent metrics" suitable system design analysis (Uday, 2014). Figure 2-2 shows the system response during a disruptive event. At the initial condition when there is no disruption, the system performance is dependent on the system reliability. When a disruption occurs at a period t_0, the system performance drops to P_y enduring the disruption and further loss in functionality (robustness). At time t_1, the system starts to recover and limits the further functional loss (rapidity). Finally, at the time t_2, resources are applied to bring the system back to full operation (Barker, 2013, Ayyub, 2014). In the context of the shipboard environment, system resilience is its ability to prevent critical system interruption and return to normal conditions after a disruptive event.

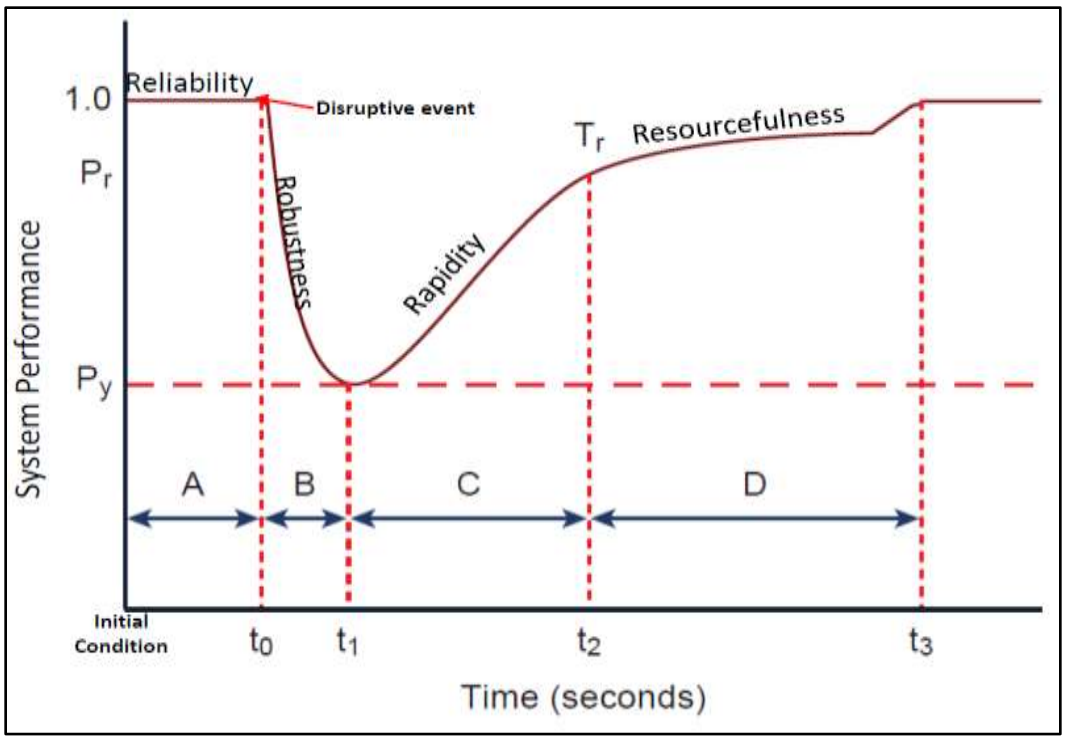

Figure 2-2: Description of resilience state transition during a disruptive event (Adapted from Henry and Ramirez-Marquez, 2012)

2.2.1 Categories of Resilience Measures

The resilience analysis approach is sub-divided into two categories: qualitative and quantitative measures. The qualitative resilience analysis examines non-numerical data such as proven methods and subject matter expert opinions. Since the praxis focuses on quantitative methods only, the interested reader is referred to Hosseini et al. (Hosseini, 2016) for a comprehensive review of the use of the qualitative method to analyze resilience.

The quantitative resilience method provides numerical descriptors and contains two sub-types, one of which involves general resilience measures that provide a quantitative means of measuring system performance without concentrating on system-specific

attributes. The general measures are further categorized as either deterministic or probabilistic measures. The deterministic approach does not account for uncertainty, while the probabilistic approach considers the stochasticity of the system behavior.

The following Sections 2.3, 2.4, and 2.5 provide a general literature review of quantitative resilience measure approaches and present examples of each model for different areas of study. In Section 2.3, the most common probabilistic resilience measures are discussed. Next, Section 2.4, covers the deterministic resilience measures. Finally, Section 2.5 discusses the traditional reliability analysis methodologies.

2.2.2 General Resilience Approaches

This praxis focuses on the probabilistic approach within general resilience measures because it provides a means of measurement of performance (MOP) of the system regardless of its structure. The probabilistic approach accords with our goal of measuring the system performance of the legacy platform and comparing it with the future platform. The probabilistic method measures the uncertainty associated with system behavior, while the deterministic method does not incorporate uncertainty. Due to the lack of data on time-dependent shipboard casualties, we employ a static function-based approach.

2.2.2.1 Probabilistic Resilience Measures

A probabilistic resilience measure depicts the stochasticity related to system performance. The literature presented below describes some of the most common resilience metrics applied to different systems, of which summary is provided in Table 2-1.

2.2.2.1.1 Earthquake Disaster Resilience Measure

Chang and Shinozuka's paper quantifies the impact of the earthquake on the technical[13], organizational[14], social[15], and economic[16] aspect of the community. It also presents a performance measurement framework that includes elements such as "robustness, rapidity, redundancy, and resourcefulness" (Chang, 2004, p.2) to quantitatively measure the disaster resilience of communities after an earthquake. This paper builds upon Bruneau's (Bruneau, 2003) work by describing resilience as the likelihood of achieving both robustness and rapidity standards during a disruptive event.

In Figure 2-5, resilience is measured by evaluating the shortfall in system performance to a pre-defined performance baseline of "robustness (r*) and rapidity (t*)." The initial loss r_o is compared with r^*, which is a pre-defined maximum acceptable system performance loss after an earthquake. The time to maximum recovery t_1, is compared to t^*, which is a pre-defined maximum acceptable disruption time. The probabilistic resilience measure quantifies the impact of impending future event by accounting for the likelihood that the system will satisfy the designed benchmark r* and t* in a given earthquake i and (2) the possibility of incidence of various seismic events. The likelihood that a system will meet the performance baseline *A* during an earthquake event of magnitude *i* is shown in Equation (2-1). Although there is some discussion of

[13] Technical resilience measures the physical system's performance when subjected to seismic activity.
[14] Organizational resilience measures the community's ability to act in response to emergencies and perform critical functions.
[15] Social resilience measures community's capability to lessen the negative social effects of loss of crucial service.
[16] Economic resilience measures the volume of direct and indirect economic losses resulting from seismic activity.

performance standards, the proper standards for disaster resilience must be identified. One benefit of this method is its wide-ranging application to other systems..

$$P(A|i) = P(r_o < r^* \, and \, t_1 < t^*) \quad (2\text{-}1)$$

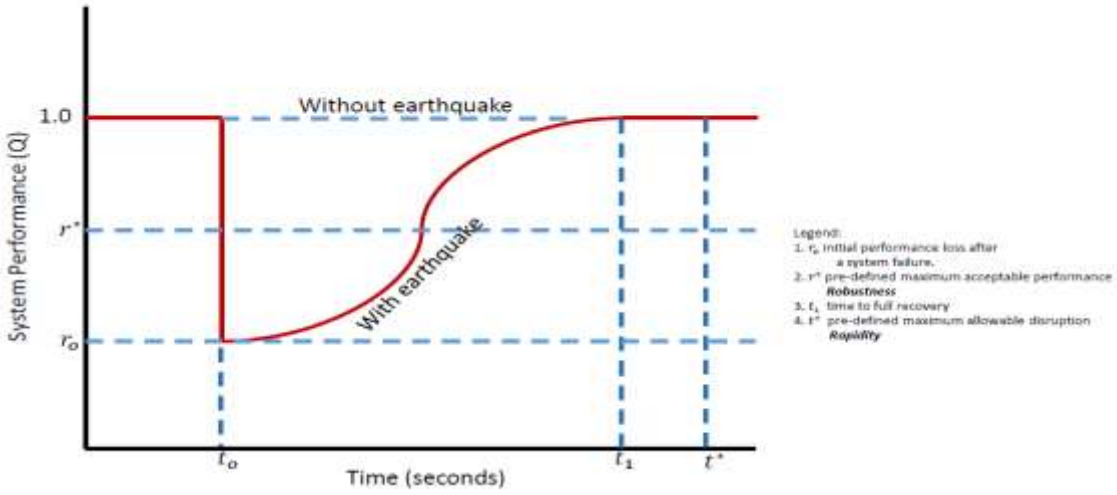

Figure 2-3: Earthquake resilience system performance measure (Adapted from Chang, 2004 p.743)

2.2.2.1.2 Time-Dependent Resilience Measure

Ouyang and Duenas-Osorio's article proposes a metric that quantifies the dynamic resilience of facilities and services that is impacted by cascading failure and system recovery. Figure 2-4 shows the system's response after the occurrence of a hazardous event. Stage 1 represents the disaster prevention stage or resistance capacity ($0 \leq t \leq t_0$). Next is Stage 2, representing the damage propagation stage or absorptive capacity ($t_0 \leq t \leq t_1$). The third stage represents the recovery stage or recovery capacity ($t_1 \leq t \leq t_E$). The time-dependent resilience $R(T)$ is measured by taking the ratio of the region bounded by $P(t)$ and the time axis $(t_o - t_1)$ to the region bounded by $TP(t)$ and the time axis $(t_0 - t_E)$. The time-dependent resilience approach is best suited for decision

support analysis on long term infrastructure improvement, modernization strategies, and life-cycle resilience analysis.

$$R(T) = \frac{\int_0^T P(t)dt}{\int_0^T TP(t)dt} \quad (2\text{-}2)$$

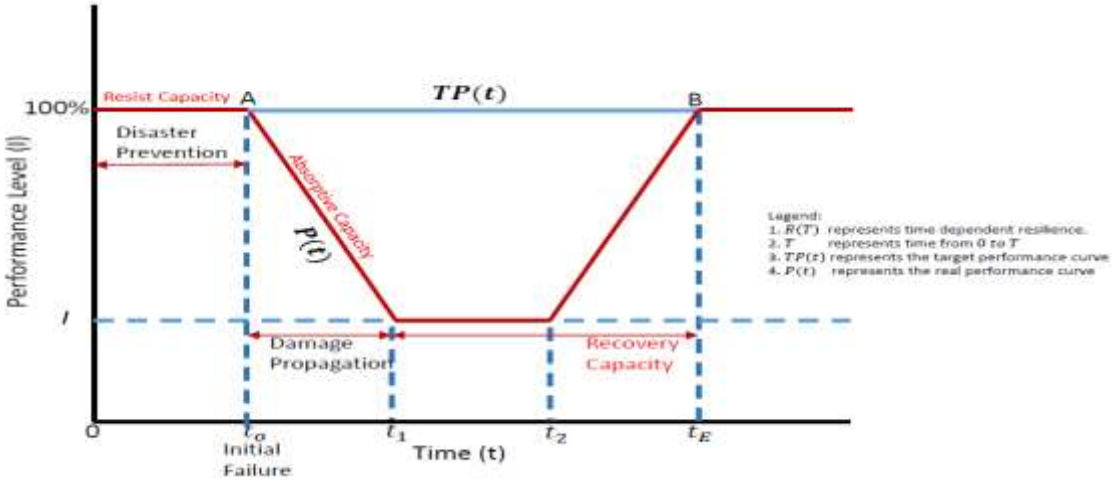

Figure 2-4: System performance after hazard event (Adapted from Ouyang, 2012, p. 2)

2.2.2.1.3 Engineered System Resilience Measure

Youn, Hu, and Wang's research applied the "Prognostic and Health Management" (PHM) model during the early design stage of an engineered system. They quantified an engineered system's resilience by transforming the "Reliability-Based Design Optimization (RBDO) framework"(Youn, 2011 p.1) to a "Resilience-Driven System Design (RDSD)" (Youn, 2011 p.1). The capacity restoration (ρ) is defined as the degree of a system's reliability recovery. The system restoration in Equation (2-3) is "a joint probability of a system failure event (E_{sf}), a correct diagnosis event (E_{cd}), a correct prognosis event (E_{cp}), and the mitigation and recovery (M/R) success event (E_{mr})". An advantage of this model is resilience is designed into individual components, that it measures both pre-disaster and post-disaster activities. However, this model does not

provide the failure mechanism and the component layout. Also, the calculation of the conditional probability can be problematic during the first disruptive event, and estimating errors caused by the subject matter expert's lack of knowledge which can result in a misleading restoration effort. Lastly, this method can only be solved by Mixed Integer Nonlinear Programming techniques.

$$\rho(R, \Lambda_{P,}\, \Lambda_{D,}\, K) \triangleq (E_{sf,}\, E_{cd}, E_{cp}, E_{mr}) \tag{2-3}$$

$$= \Pr(E_{mr}|E_{cp}E_{cd}E_{sf}) * \Pr(E_{cp}|E_{cd}E_{sf}) * \Pr(E_{cd}|E_{sf}) * \Pr(E_{sf})$$

$$= K * \Lambda_P * \Lambda_D * (1\text{-}R)$$

where $K, \Lambda_{P,}\, \Lambda_D$ represents the conditional probabilities of M/R

(1-R) represents the probability of system failure

Therefore:

$$\textit{Resilience } (\Psi) = \textit{Reliability } (R) + \textit{Restoration } (\rho) \tag{2-4}$$

2.2.2.1.4 Resilience Measures with Degradation as a Function of Time

Ayyub's work suggests a resilience metric that considers the effects of aging on failure episodes with a frequency rate (λ) based on a Poisson process. The graph in Figure 2-5 depicts the system performance (Q) and the estimated performance with aging effects. The proposed resilience metrics are shown in Equations (2-5) through (2-8). The failure-profile (F) depicts the metrics for "*robustness* and *redundancy*,"(Ayyub, 2014, p.346) while the recovery-profile (R) depicts the metrics for "*resourcefulness* and *rapidity"*(Ayyub, 2014, p.346). The time to failure (T_f) is characterized by the system probability density function (PDF), as shown in Equation (2-8). Ayyub's model is

associated with several advantages compared to the other resilient studies in this paper: the model 1) shows the relationship between reliability and risk, 2) provides means of measuring economic valuation and business case analysis, and 3) advocates both mitigation and contingency strategies. A disadvantage is that the model considers all components to be independent and does not relate component performance to system-level performance.

$$Resilience\ (R_e) = \frac{T_i + F\Delta T_f + R\Delta T_r}{T_i + \Delta T_f + \Delta T_r} \tag{2-5}$$

$$Failure(F) = (\int_{t_i}^{t_f} f(dt))/(\int_{t_i}^{t_f} Q(dt)) \tag{2-6}$$

$$Recovery(R) = (\int_{t_f}^{t_r} r(dt))/(\int_{t_f}^{t_r} Q(dt)) \tag{2-7}$$

$$T_f = -\frac{d}{dt}\int_{S=0}^{\alpha} \exp[-\lambda t(1 - \frac{1}{t}\int_{t=0}^{t} F_L(\alpha(\tau)s)dt]f_{s_0}(s)ds \tag{2-8}$$

where F_L represents the CDF of L

f_s represents the PDF of S

α_t represents the aging as a function of time *t*

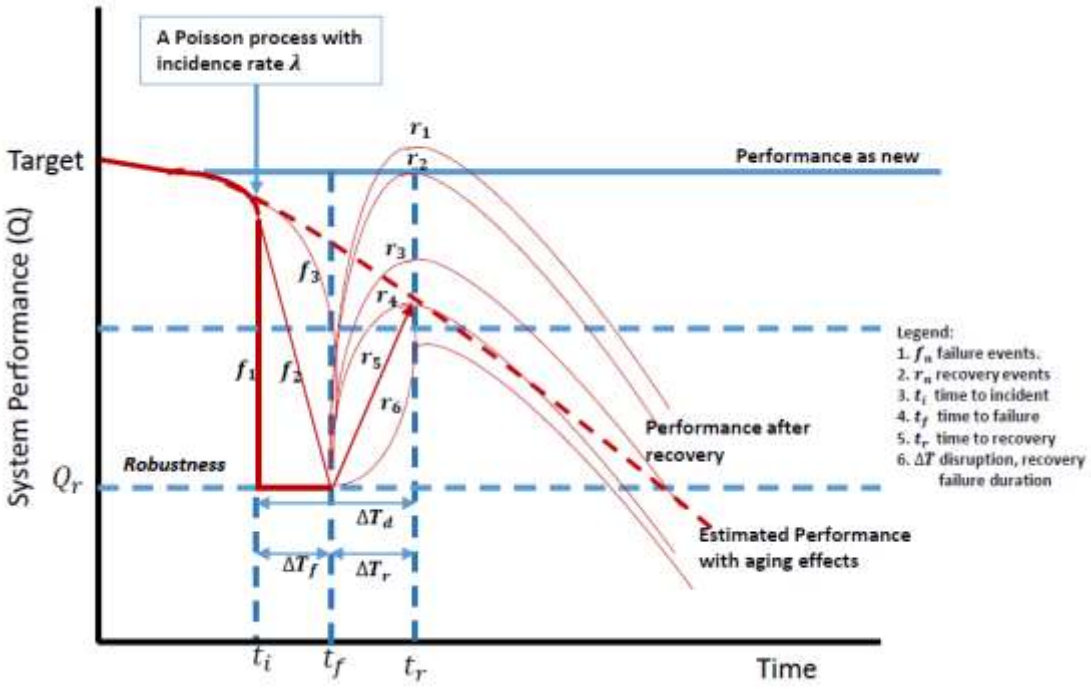

Figure 2-5: System resilience with aging effects (Adapted from Ayyub, 2014 p.347)

2.2.2.1.5 Network-Based Resilience Measure

Franchin and Cavalieri's work presents a probabilistic resilience measure using network theory with a Bayesian Network network representation. System resilience is based on the comparison of road network efficiency before and following the disruptive event. The infrastructure efficiency is defined as a reciprocal proportion to their shortest route. In Equation (2-9), the resilience metric R is computed by taking the inverse of the dislocated popultion (P_d) is the portion of the dislocated and the road network efficiency before the earthquake (E_o), then multiplied by the recovery curve of the fraction of the displaced population (EP_r). The value of resilience is normalized between zero and one [0, 1].

$$R = \frac{1}{P_d E_o} \int_0^{P_d} E * P_r \, dP_r \quad (2\text{-}9)$$

The Bayesian network model is used to simulate the model by using Monte Carlo and importance sampling simulation technique. The nodes denote a random variable, and the link denotes the interdependence among the random variables, which form a network showing their joint probability distribution. An advantage of this model is the evaluation of the dependencies among critical infrastructure systems using graph theory. Additionally, the resilience metric is pertinent to other facilities such as the energy and water systems.

Table 2-1: Probabilistic Quantitative Resilience Measures

	Resilience Measures	Author	TItle	Area of Study	Measurement Technique	Interdependence Measure	Knowledge Gap
P r o b a b i l i s t i c	1.Conceptual (Technical, Organizational, Social, Economic) 2. Performance (Robustness, Rapidity, Redundancy, Resourcefulness)	S.E Chang, M. Shinozuka, Earthquake Spectra, 20 (3) (2004), pp. 739-755 DOI: 10.1193/1.1775796	"Measuring improvements in the disaster resilience of communities"	Disaster	Integration	NO	Domain specific measure. Performance standards needs to be identified.
	Time-dependent metric. R(T) Disaster Prevention, Damage Propagation, Recovery	M Ouyang, L Duenas-Osorio, Chaos 22, 033122 (2012), pp 1-11 DOI: 10.1063/1.4737204	"Time dependent resilience assessment and improvement of urban infrastructure systems"	Infrastructure	Integration	NO	Domain specific measure.
	Resilience measure is the sum of reliability (R) and restoration(p). This framework designs systems with resilience charactersitics	B.D. Youn, C. Hu, P. Wang, Journal of Mechanical Design, 133 (2011), p. 10	"Resilience driven system design of complex engineered systems"	Engineering Design	Conditional probability	NO	Measures individual component resilience only, not system-wide resilience
	Measures system performance with effects of aging. Failure is a measure of Robustness and Redundancy. Recovery is a measure of Resourcefulness and Rapidity.	B.M. Ayyub, Risk Analysis, 34 (2) (2014), pp. 340-355, DOI: 10.1111/risa.12093	"Systems resilience for multihazard environments: Definition, metrics, and valuation for decision making"	Community and System	Integration	NO	Does not relate component performance to system level performance
	Applies Network Theory and Bayesian Network. The efficiency between 2 nodes is inversely proportional to their shortest distance	P. Franchin, F. Cavalieri, Computer-Aided Civil and Infrastructure Engineering, 30 (7) (2015), pp. 583-600 DOI: 10.1111/mice.12092	"Probabilistic assessment of civil infrastructure resilience to earthquakes"	Community	Monte Carlo Simulation	YES	BN is susceptible to state explosion.

2.2.2.2 Deterministic Resilience Measures

A deterministic resilience measure is used to estimate system resilience in response to a specific disruption without uncertainty (i.e., the probability of disruption) in the metric. The literature below describes some of the most common deterministic measures, and a summary is provided in Table 2-2.

2.2.2.2.1 Resilience Triangle Method

The research of Bruneau et al. proposed a new measure of seismic resilience called the resilience triangle model, which is shown in Figure 2-6 (Bruneau, 2003). This method compares the quality of service (QoS) of the damaged infrastructure after seismic events to the baseline QoS (100%). A higher value of resilience loss (*RL*) indicates inferior resilience. A small value of resilience loss (*RL)* value implies better resilience. The parameter *Q(t)* measures the QoS of the infrastructure, which varies with time (*t*). The infrastructure system's performance is between 0% to 100%, where 100% signifies that there is no reduction in service and 0% signifies that the service is unavailable. System restoration is expected to occur over the period extending from time t_0 to t_1. Resilience is defined by Equation (2-10).

$$R = \int_{t0}^{t1}[100 - Q(t)]dt \qquad (2\text{-}10)$$

Moreover, resilience is characterized by the following four attributes: "1) robustness, 2) redundancy, 3) resourcefulness, and 4) rapidity" (Bruneau, 2003 p.737). Some weaknesses of this method are that 1) the area under the curve (RL) is difficult to measure since the time of disruption is instantaneous, and recovery starts immediately, 2) the QoS of the infrastructure's data must be measured over time to develop the correct

model, and 3) the assumption that QoS is 100% operational prior to the earthquake is unrealistic. However, this method includes several advantages, such as its general applicability and the fact that the model can be employed for many systems.

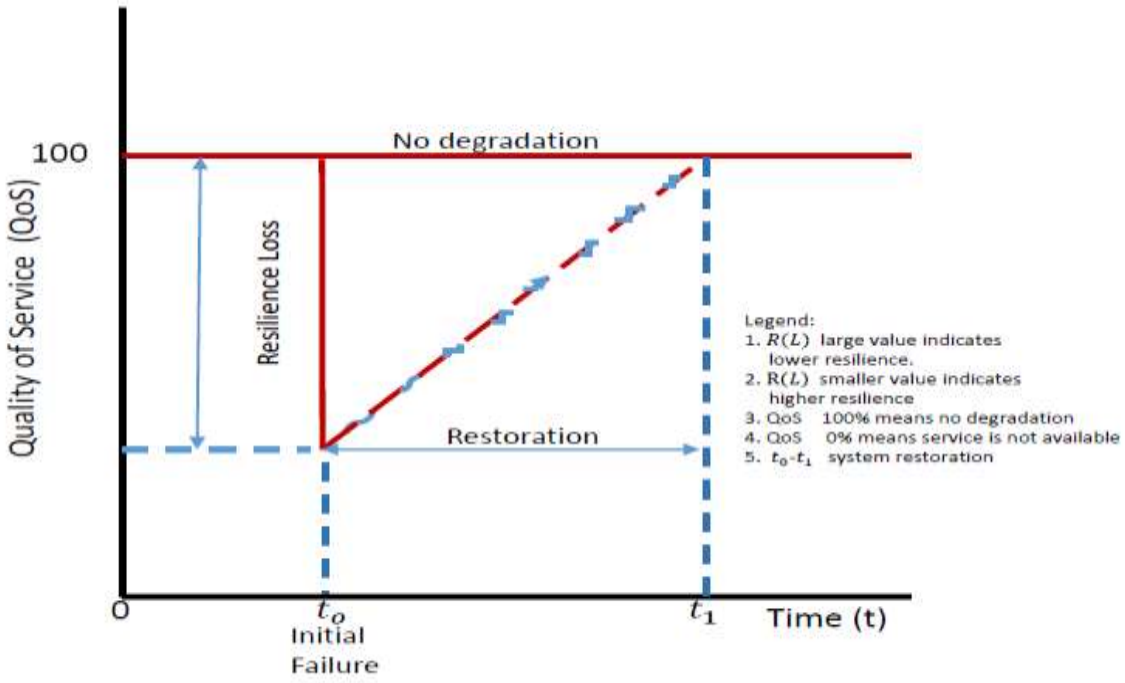

Figure 2-6: The resilience triangle method (Adapted from Bruneau, 2003 p.737)

2.2.2.2.2 Predicted Resilience Method

Zobel's paper presents a predicted resilience method that improved Bruneau's resilience triangle model (Zobel, 2011). The predicted resilience of a system is a function of the estimated initial loss (X) and the accompanying recovery time (T) for a future disaster event. Recovery time T represents the rapidity measure, while $(1 - X)$ represents a measure of robustness, as shown in Figure 2-7. This method demonstrates the logical connection between the first impact of disruption and the subsequent recovery time from a disaster. In Equation (2-11), X represents the percentage of functionality initially lost

due to the impact of disruptive events, T accounts for the time to recovery, and T* is the larger area from which triangle area XT/2 is subtracted. Although the predicted resilience triangle method is simple to apply, the linear recovery that it assumes is unrealistic. However, this model allow decision makers to estimate losses, determine recovery time, and plot the predicted and adjusted resilience curves that can be used for trade studies (Zobel, 2011).

$$R(X,T) = 1 - \left(\frac{XT}{2T^*}\right) \tag{2-11}$$

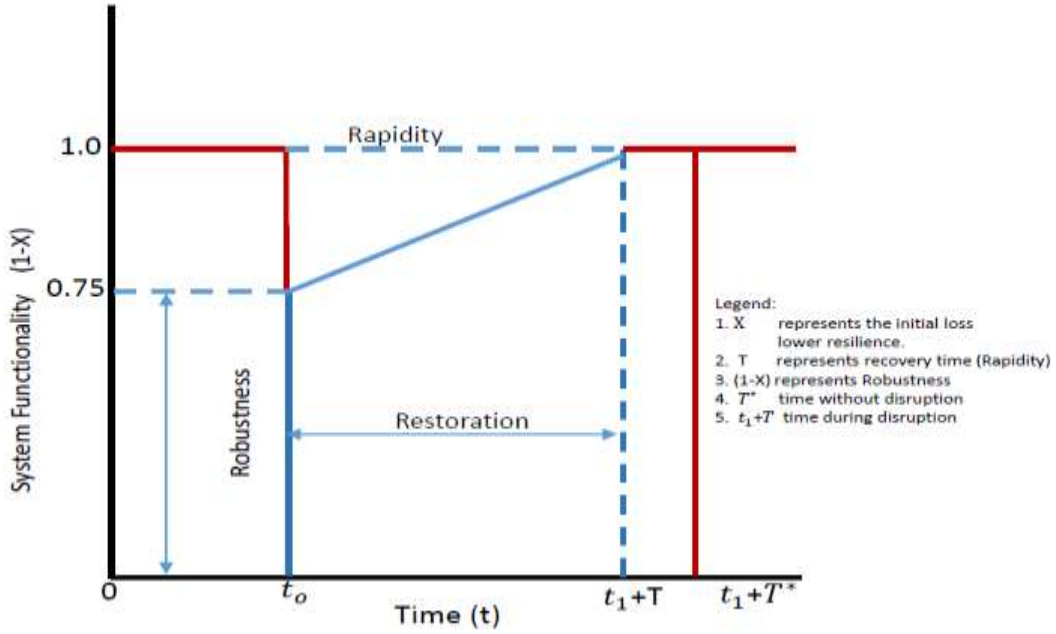

Figure 2-7: The predicted resilience triangle as a proportion of T* (Adapted from Zobel, 2011 p. 396)

2.2.2.2.3 Economic Resilience Model

Rose's work proposes a static economic resilience model, as depicted in Figure 2-8 and Equation (2-12) (Rose, 2007). This concept focuses on the efficient distribution of capabilities at period *T* which quantifies the proportion of the expected reduction in

function level to the worst case degradation. One drawback of this approach is the difficulty of estimating the expected degradation performance levels, particularly for an unknown disruption, that cannot be accurately estimated.

$$R = \frac{\%\Delta Y^{max} - \%\Delta Y}{\%\Delta DY^{max}} \quad (2\text{-}12)$$

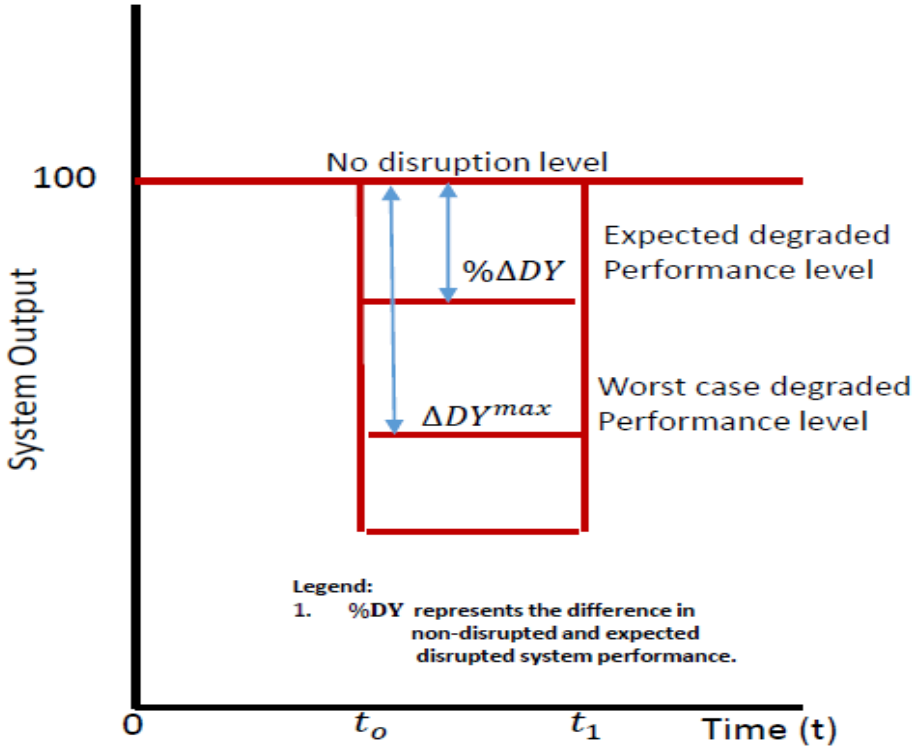

Figure 2-8: Static economic resilience (Adapted from Rose, 2007)

2.2.2.2.4 State Transition Resilience Measures

Henry and Ramirez-Marquez paper presents a "time-dependent metric" (Henry, 2012, p.117) that measures system resilience as shown in Figure 2-9. In Equation (2-13), the numerator represents the system recovery period (t) while the denominator represents the entire damage because of the disruptive event (e^j). An advantage of this model is that it

provides a general resilience measure and use of the figure of merit (FOM) to measure system resilience. A disadvantage is that system functions and figure of merit needs to be identified depending on the system under evaluation.

$$\mathcal{R}esilience(t|^{e^j}) = [\varphi(t|e^j) - \varphi(t_d|e^j)]/[\varphi(t_o) - \varphi(t_d|e^j)] \quad (2\text{-}13)$$

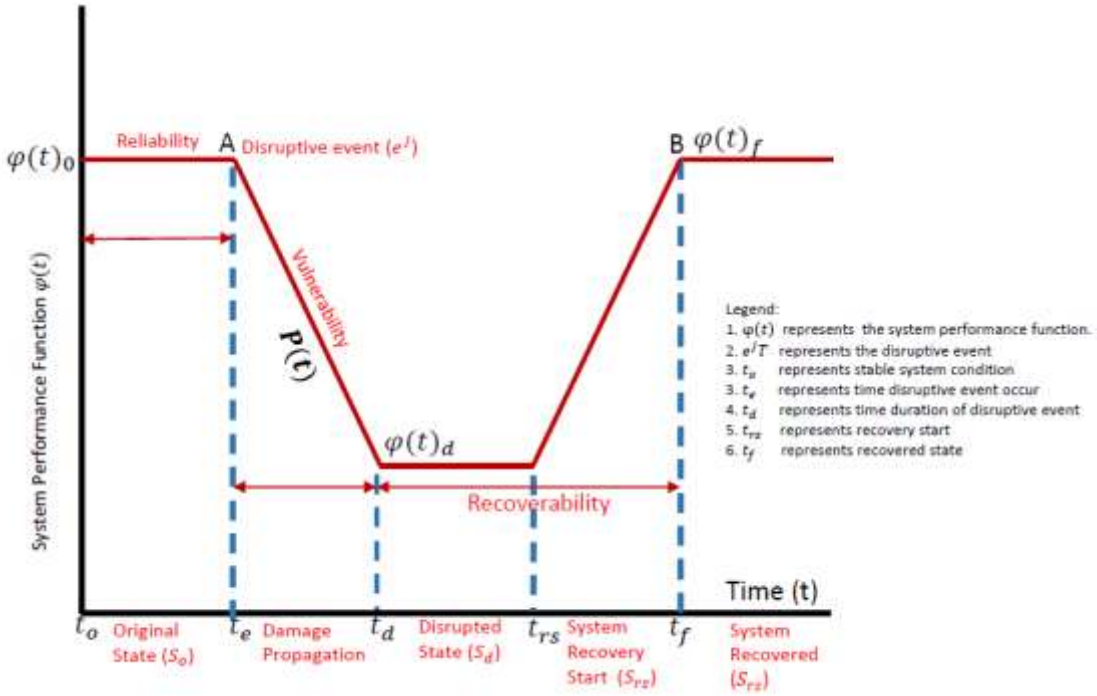

Figure 2-9: State transition resilience measure (Adapted from Henry, 2012 p. 117)

2.2.2.2.5 Organizational Resilience Measures

Organizational resilience is crucial for the social and economic sustainment after any disruptive events. Omer et al. proposes a means of quantifying organizational resilience by using graph theory and social network analysis method. The organizational resilience measure, shown in Equation (2-14), is measured by comparing network closeness centrality before shock (C_{CBS}) and closeness centrality aftershock (C_{CAS}). Figure 2-10

shows the organizational model and the nodal interdependence (Omer, 2014). An advantage of this paper is that it shows the logical and physical architecture within the organization that allows management to design organizational resilience. However, in order to design organizational resilience, the affected systems and sub-systems must be carefully mapped-out and analyzed.

$$R_{cc} = \frac{C_c(v)_{before\_shock}}{C_c(v)_{after\_shock}} \quad (2\text{-}14)$$

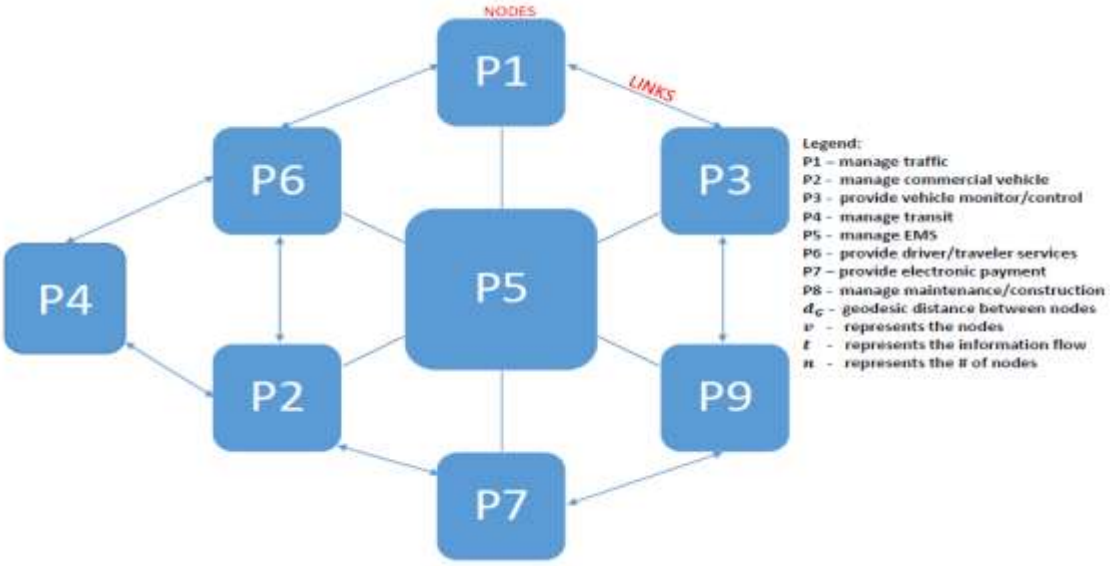

Figure 2-10: Organization network model (Adapted from Omer, 2014 p.569)

2.2.2.2.6 Human and Machine System Resilience Measures

The research of Enjalbert et al. research proposes a method by which to measure machine and human system resilience (Enjalbert, 2011). This metric quantifies the public transport's human and machine interdependence. Figure 2-11 shows the system response during a disturbance. The baseline represents the 100% safe condition before the disturbance. The "minimum acceptable threshold" (Enjalbert, 2011 p.338) represents the

standard design safety level. E_{max} represents the disturbance's maximum impact on system safety, and E_j is the initial disturbance at time T_j. Enjalbert et al. (Enjalbert et al., 2011) resilience model measure the local resilience shown in Equations (2-15) and global resilience shown in Equation (2-16). This paper studies the human behavior while driving the transport system and measures the HMS performance.

$$Local\ Resilience = dS(t)/dt \tag{2-15}$$

$$Global\ Resilience = \int_{t_b}^{t_e} dS(t)/dt \tag{2-16}$$

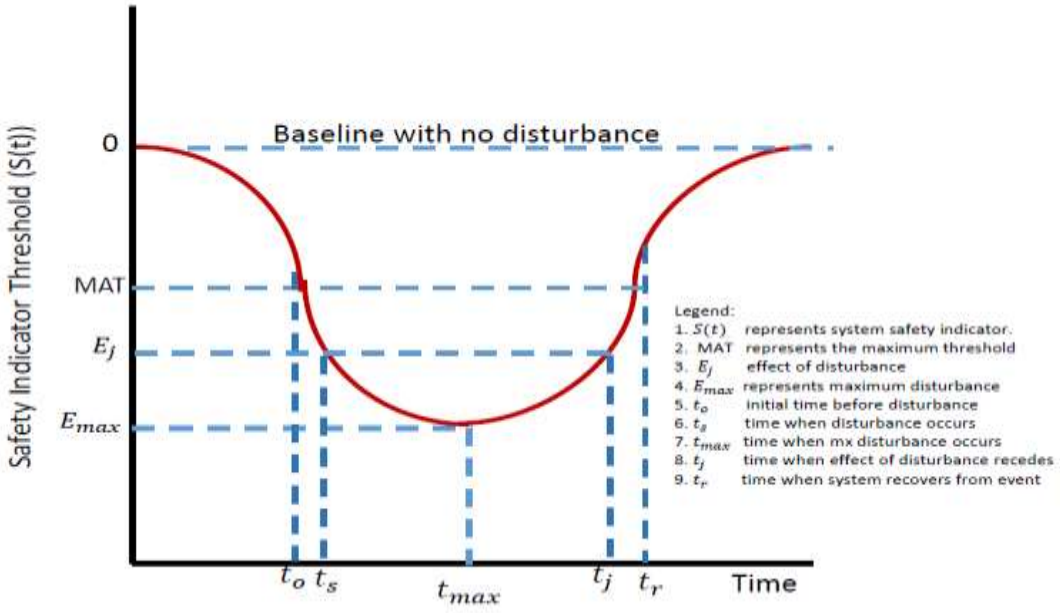

Figure 2-11: Resilience measure (Adapted from Enjalbert, 2011 p. 338)

Table 2-2: Deterministic - Quantitative Resilience Measures

	Resilience Measures	Author	TItle	Area of Study	Measurement Technique	Interdependence Measure	Knowledge Gap
D e t e r m i n i s t i c	Resilience Triangle Method has 4 attributes: Robustness, Redundancy. Resourcefulness. Rapidity	M Bruneau, S.E Chang, R.T Eguchi, G.0 Lee. T.D O'Rourke, A.M Reinhom, M Shinozuka, K Tierney, W.A Wallace, D Von Winterfeldt Earthquake Spectra. 19 (4) (2003), pp. 733-752 DOI: 10.1193/1.1623497	"A framework to quantitatively assess and enhance the science the seismic resilience of communities"	Civil infrastructure	Integration	NO	Area under the curve (RL) is difficult to measure since the time of disruption is instantaneous.
	Predicted Resilience Triangle Method	C.W. Zobel, Decis Support Syst, 50 (2) (2011), pp. 394-403 DOI: 10.1016/j.dss.2010.10.001	"Representing perceived tradeoffs in defining disaster resilience"	Disaster	Algebraic	NO	Linear recovery that it assumes is unrealistic.
	Static and Dynamic economic resilience model	A. Rose, Environ Hazard, 7 (4) (2007), pp. 383-398, DOI: 10.1016/j.envtiaz.2007.10.001	"Economic resilience to natural and man- made disasters: multidisciplinary origins and contextual dimensions"	Economics	Algebraic	NO	Difficult to estimate the expected degradation of performance levels
	State Transition resilience model. Measures reliability, vulnerability and Recoverability. Resilience is measured as the ratio of recovery time to loss suffered.	D Henry, J.E. Ramirez-Marquez Reliab Eng Syst Saf, 99 (2012), pp. 114-122 DOI: 10.1016/j.ress.2011.09.002	"Generic metrics and quantitative approaches for system resilience as a function of time"	Transportation	Algebraic	NO	Need to identify or develop system functions and figure of merit in advance.
	Resilience metric based on Closeness Centrality. Closeness centrality is used to measure organizational resilience.	M Omer, A Mostashari, U. Lindemann Procedia Computer Science, 28 (2014), pp. 565- 574 DOI: 10.1016/j.procs.2014.03.069	"Resilience analysis of soft infrastructure systems"	Software Infrastructure	SNA	YES	Challenges in mapping the organizational relationships.
	Human and Machine system resilience	S. Enjalbert, F. Vanderhaegen, M. Pichon, K. A. Ouedraogo, P. Millot, Springer-Verlag Italia Srl (2011), pp. 335-341	"Assessment of transportation system resilience"	Transportation Safety	Integration	YES	Chalenges in deterrmining human-machine dependencies

2.3 Traditional Reliability Analysis Methods

Currently, reliability analysis is a fundamental component of designing systems that are associated with safety and critical application requirements such as nuclear plants, space shuttles, and naval vessels. Rapid innovations in technology have made it easier for system designers to integrate various CPSs seamlessly. However, the integration of hardware and software has led the components to exhibit emergent behavior, and component or system interdependence is becoming more challenging to model and analyze using traditional quantitative methods (Madni, 2009). System engineers thus depend solely on commercially available quantitative analysis software tools to assess system reliability.

2.3.1 Fault Tree Analysis

Various probabilistic risk assessment (PRA) methodologies are available to model and perform system analysis. Table 1 presents the most commonly used methods and the advantages, disadvantages, and limitations of each. FTA is one of the most broadly recognized methods for reliability analysis (Boudali, 2005). It is a deductive technique in a graphical format that provides a logical illustration of the possible failure occurrences which can result in an unfavorable consequence (Lewis, 1996). Fault tree analysis can combine the sources of equipment and human failures wherein the most severe outcome is chosen as the top failure event for a system (Lewis, 1996). The top events are usually failures of significant consequences that can result in a significant safety hazard, potential economic loss, or loss of life. Some of the advantages of the Fault Tree analysis are 1) it is easy to use, 2) presents an intuitively logical representation or abstraction of the system, and 3) it is remarkably successful at identifying potential causes of accidents or

system failures (Boudali, 2005 p.1; Lewis, 1996 p. 376). Some of the drawbacks of fault tree analysis are 1) its inability to deal with component interdependencies (Boudali, 2005), 2) complex fault tree is difficult to understand and bears no resemblance to system flow sheets, and 3) it is not mathematically unique (Henley, 1981).

2.3.2 Bayesian Network

The Bayesian network (BN) uniquely describes a joint probabilistic distribution model of all the random variables present in the graph that contains nodes and links (Boudali, 2005). The nodes correspond to the random variables and the links or edges correspond to the dependencies among the nodes (Boudali, 2005). The BN has become one of the most prevalent reliability and risk analysis model for complex systems (Khakzad, 2013). Applying the conditional independence theorem and the Chain Rule, Equation (2-17) shows a joint probability distribution that is decomposed as the product of the likelihoods of the nodes given their sample set.

$$P(X) = \prod_{i=1}^{n} P(B_i|P_b(B_i)) \quad (2\text{-}17)$$

Where: P(X) represents the distribution of variables that occur at the same time

$P_b(B_i)$ represents the sample set of variable B_i

BN takes advantage of Bayes Theorem to update the likelihood of trials given a new measured data, called evidence E, to yield the posterior probability in Equation (2-18):

$$P(X|E) = [P(X)\ P(E|X)]/P(E) \quad (2\text{-}18)$$

The advantages of BN are 1) a robust method to model qualitative and quantitative dependencies [Khakzad, 2013], 2) superior modeling and analytical capabilities for complex systems (Boudali, 2005), and capable of addressing partial

failures [Uday, 2015]. However, the BN has several shortcomings 1) it is not suited to model closed-loop processes, and 2) learning and updating the model requires a significant computational load [Uusitalo, 2007].

2.3.3 Markov Analysis

The Markov Analysis (MA) is a modeling technique for systems with state[17] transitions and computing the probability of achieving several system states from the model. The MA is a graphical modeling tool that use state transition diagrams[18] to evaluate the complex systems components that have timing, queuing, repair, redundancy, and fault tolerance issues (Ericson, 2016). The MA is based on the Markov Chain (MC[19]) concept that is a standard way to model random or stochastic processes[20]. The transition matrix represents the probability distribution of the state transition. For example, a Markov Chain that has Q possible states will have a Q x Q matrix whose entries in each row must add up to precisely 1; each row represents its probability distribution. There are several advantages when using the MA technique 1) provides precise model representation for complex system design, 2) great tool for modeling and understanding system failure and repairs, and 3) can identify safety issues during the design process (Ericson, 2016). There are several significant shortcomings: 1) the manual generation of system behavior is tedious and predisposed to error when

---

[17] State. "The condition of a component or system at a particular point in time such as operational state, failed state, degraded state, etc." (Henley, 2016 p.431)
[18] State transition diagram. "It is a directed graph representation of system states, transition between states, and transition rates that contains the information for developing the state equations" (Henley, 2016 p.432).
[19] Markov Chain. "These are sequences of random variables in which the future variable is determined by the present variable, but independent of history" (Henley, 2016 p.432).
[20] Stochastic process. "It is a model that predicts a set of possible outcomes weighted by their likelihoods or probabilities" (Henley, 2016 p.432).

developing the model, 2) it is susceptible to the state explosion[21] problem due to the exponential growth of the states related to the number of system components (2^n) (Busic, 2012), 3) it does not identify system hazard and root cause (Ericson, 2016).

Table 2-3: Comparison of Traditional Reliability Methods

Method	Characteristics	Advantages	Disadvantages	Limitations
Fault tree analysis (FTA)	1. Starts with event initiation and identifies the causes of failures, using Boolean logic to lead to the top event (TE). 2. Examines the alternative sequence. 3. Identifies the weakest component.	1. Well-accepted. 2. Great for identifying failure relationships. 3. Seeks ways to fail. 4. Identifies gross effect sequences and alternative consequences of failure.	1. Large fault trees are complex and require a computational method. 2. Not mathematically unique. 3. Fails in parallel sequence. 4. Dependence modeling is difficult to understand. 5. A complex system requires a computerized algorithm.	1. Cannot handle partial failures as seen in SoS. 2. Results in substantial and complicated design guidance, making it less likely to be useful. 3. Does not address design changes.
Bayesian network (BN)	1. A graphical representation of the joint probability of random variables. 2. The BBN is a technique used for knowledge representation and reasoning under uncertainty, representing a joint probability distribution.	1. Models the joint distribution of random variables. 2. Predicts and estimates the conditions of the random variables. 3. Handles a large number of TEs. 4. Predictions are amenable to risk analysis.	1. Not suitable for SoS modeling. 2. BN update in maximum-k is NP-hard[22] to approximate when k≥ 3. 3. Potential to over-emphasize expert opinion. 4. Large BN/BBNs can become unmanageable. 5. BBNs behave rigidly to unforeseen events.	1. It considers only binary failures. 2. Not suitable for SoS modeling. 3. Less suitable for unidirectional relationships.
Markov Analyses	1. Extensive use for dependability analysis of dynamic systems.	1. Versatile tool for the complex modeling system. 2. Well-established method.	1. Manual development of Markov chain system behavior is a daunting task. 2. Prone to error.	1. Requires extensive memory to store conditional probabilities resulting in state explosion. 2. Limits the number of dependencies.

[21] State space explosion. "It is a phenomenon when using the Markov Chain when the number of states that is required to accurately describe the dynamics of such a system grows exponentially with respect to the dimensions of the system" (Henley, 2016 p.432).
[22] NP hard. A "Non-Deterministic Polynomial-Time Hardness" that defines the property of a class of problems that are, least as hard as the hardest problems in NP (Arora, 1998).

2.4 Applying Network Theory to Analyzing Complex Systems

For many years, complex networks such as the Internet, molecular biology, and metabolic and protein interaction networks were difficult to describe and understand due to their complex topology. The study of networks predates 1736 with Leonard Euler's solution to the Konigsberg bridge problem (MAA, 2018). Between the 1950s and 1960s, a theoretical model called a random graph, with a highly skewed distribution, was developed by Solomonoff and Rapoport (Solomonoff, 1951) and Erdos and Renyi (Erdos, 1959; 1960; 1961) to describe network structures. The Solomoff and Rapoport paper demonstrated the crucial property of the model: "as the ratio of the number of edges to nodes in the graph increased, the network reaches a point at which it undergoes an abrupt change from a collection of disconnected nodes to a connected state in which the graph contains a giant component" (Newman, 2006 p.11). Erdos and Renyi's papers demonstrated that many properties of the random graph emerge suddenly when enough edges are added to the graph.

An area of physics studies closely related to random graph theory is percolation theory, the introduction of which by Simon Broadbent and John Hammersley during the late 1950s revolutionized oil exploration and superconductivity (Broadbent, 1957). The bond percolation models study the system properties in which the bonds on the lattice or network are either occupied or not with some occupation probability p, thus resulting in a spanning cluster. The methods developed for the random graph can be applied to percolation theory as well.

While graph theory and percolation theory were being developed, Pool and Kochen's paper "Contacts and Influence" (Pool, 1978) developed the SNA as an application of the

random graph, using the small-world effect phenomenon in scientific terms for the first time. The authors formulated the social network attributes such as the acquaintance volume, degree distribution, degree influence, and network structure. This paper influenced Travers and Milgram, who published their related work, "An experimental study of the small-world problem" (Travers, 1959).

Between 1974 and 1986, the mainframe computer was transformed into personal computers, while memories and computer chips were rapidly miniaturized and 32-bit architecture was introduced (Zimmermann, 2018). These factors, as well as the Internet explosion, led to the recent interest in network science research. Various empirical studies have shown that real networks are different in their structure compared to the simple random graph mathematical network models. For example, Watts and Strogatz's paper introduced the "small world" model into the social network structure. These paper introduced two properties, namely, shortest path[23] and clustering or transitivity (Watts, 1998). Barabasi and Albert's paper introduced both the power law degree[24] or scale-free distribution[25] in networks and the preferential attachment model[26] (Barabasi, 1999). Albert, Jeong, and Barabasi's paper presented the path length for the World Wide Web and showed that it has power-law degree distribution (Albert, 1999). In their research, Broder et al. divided the structure of the World Wide Web into four regions: giant

[23] Shortest path: the shortest path distance $d(m,n)$ is the quantity of links in the shortest path between the nodes m and n in a graph.
[24] Power law degree: a functional relationship between two measures, where a relative change in one measure results in a relative change in the other measure, independent of the initial size of those measures: one measure changes as a power of another.
[25] Scale free distribution: a feature of entities that do not change in measures when multiplied by a common factor, thus representing a universality.
[26] Preferential attachment model. Barabasi and Albert suggested that vertices gain new edges (World-Wide-Web, citations, etc.) in proportion to the number they already have.

strongly connected (28%), links in (21%), links out (21%), and other components and tendrils (30%) (Broder, 2000). Finally, the paper by Faloutsos et al. found that the Internet is a scale-free network with a power-law degree distribution.

Barabasi and Albert (1999) introduced the scale-free network, a distribution in which the probability of finding a node decay is a negative power of the degree $p(k) = k^{-\gamma}$. This equation means that the likelihood of locating a high-degree node is relatively small compared to the likelihood of finding low-degree nodes. Scaling the degree-k by a constant factor *c* results in the proportional scaling function shown below:

$$p(k, c) = A(ck)^{-\gamma} = Ac^{-\gamma} * p(k) \quad (2\text{-}19)$$

Since the power law relationship is usually plotted on the log scale obtaining a straight line, the following equation is valid:

$$p(k) = -\gamma ln\, k + \ln A \quad (2\text{-}20)$$

Multiplying with a scale factor *c* suggest that only the y-intercept of the straight line changes but the slope *c* is always the same. This phenomenon is called self-similarity[27] (Barabasi, 1999). The scale-free network offers a credible explanation of the growth dynamics, topology, and characteristics of complex networks.

Recent studies have focused on the robustness of networks to random or direct attacks. Albert, Jeong, and Barabasi's paper discussed the network resilience of random graphs and scale-free networks. The paper concludes that the scale-free network is more

[27] "Self-similarity. It is a typical property of artificial fractals. For example, scale invariance is an exact form of self-similarity where at any magnification there is a smaller piece of the object that is like the whole; parts of the object show the same statistical properties at many scales" (Serrano, 2008).

robust to the random removal of nodes but is highly fragile to directed attacks (Albert, 2000). Cohen, ben-Avraham, and Havlin's research papers on the resilience of the internet to random and direct attack use percolation theory to provide an exact value for the phase transition p_c that must be removed before the network disintegrates (Cohen, 2000). The authors derived the following formula after the removal of degree-k nodes, where: k_o represents the initial degree-k while k represents the new degree-k after node removal; and $P(k_o)$ represents the original degree distribution while $P'(k)$ represents the new degree distribution after removal of a fraction of nodes p.

$$P'(k) = \sum_{k_0=k}^{\alpha} P(k_o) \binom{k_o}{k} (1-p)^k \, p^{(k_o-k)} \tag{2-21}$$

Molloy and Reed's mathematical expression shown below explains that for a network to have a spanning cluster[28], the average degree (refers to the left-hand side of the equation) of a cluster must be equal to two, where: m, n are nodes, and $P(k_m|m \leftrightarrow n)$ represents the joint probability that node m has a degree k_m , given that node m is connected to node n (Molloy, 1995).

$$\sum_{k_m} k_m \, P(k_m|m \leftrightarrow n) = 2 \tag{2-22}$$

Using equation (2-21) and (2-22), the percolation threshold p_c is solved by using the first moment or average degree $< k_o >$ and second moment or variance degree $< k_o^2 >$ resulting in equation (2-23):

[28] Spanning cluster or giant component: a terminology used in random graph used to describe groups of nodes with size equal to the whole network.

$$p_c = \frac{1}{\frac{<k_o{}^2>}{<k_0>}-1} \quad (2\text{-}23)$$

The authors presented the impact of removing fractions of nodes on the spanning cluster or size of the giant component by plotting the fraction of nodes that remain in the spanning cluster after the breakdown of a fraction *p* of all nodes concerning the fraction of *p*. The percolation theory is further discussed in Section 3.2

2.6 Summary

In this praxis, numerous approaches for measuring the resilience of complex and interdependent systems have been studied (Francis, 2014; Uday, 2015; Woods, 2015; Hosseini, 2016; Nan, 2017). Although resilience is a well-known concept, the diversity of its application makes it difficult to identify a particular resilience metric (Francis, 2014; Uday, 2015).

A literature search of 75,499 publications concerning resilience revealed only a small proportion of resilience-related research in the engineering domain, including only 25 research papers in "resilience and percolation," with four publications dedicated to the application of percolation in networks and a few papers about resilience in maritime systems (Song, 2016). A significant knowledge gap thus exists in understanding the resilience of the maritime system and the influence of resilience on system design. Based on the knowledge gap identified from the literature reviews, this praxis will develop a percolation-based metric framework to measure the system resilience and efficiency. The validity of the model is paramount; thus, the author will use published power grid data as a baseline and for comparison of systems. The author will use Minitab for a statistical test.

Chapter 3: Research Methods

The critical infrastructures are more reliant on communication systems to provide monitoring and control signals. Nowadays, due to the system dependencies, the critical infrastructures are more susceptible to stochastic disaster-based breakdowns. To minimize the impact of these disruptive events, there is a necessity to develop a resilient and efficient communication systems. In this section, we briefly discuss the percolation-based metric framework, the data set collection and preparation process, the method for calculating system resilience (robustness), and the method for calculating communication efficiency. The percolation and SNA approaches are applied to quantify resilience and efficiency. The power grid and the maritime platforms (legacy and future versions) are used as case studies to show the utility of the percolation-based metric.

3.1 Percolation-Based Metric Framework

When designing communication systems, various systems are analyzed to determine which is best. One means of comparing these solutions is to generate a rank order resilience of the system proposals by measuring resilience (robustness) and efficiency. Figure 3-1 illustrates the percolation-based metric framework applied in this praxis. The framework uses the combined application of percolation and social network theories to analyze the communication system's resilience and efficiency. The framework starts with the input, during which the raw data from the maritime platform's FIRD is transformed into a usable format for the Gephi software. The Gephi software, an SNA software, provides the centrality measures data such as degree centrality and closeness centrality, which are the parameters required in the calculation processes section.

The calculation processes section is the period during which the computations for the robustness (fragmentation threshold (f_c)) and efficiency ($E(G)$) are performed. An Excel spreadsheet is used to calculate the communication system's fragmentation threshold for each node, and likewise for the communication efficiency. The random removal of all nodes is simulated, and thirty stochastic simulations are conducted. There are 329 nodes in the Italian power grid, 783 nodes in the legacy maritime platform, and 920 nodes in the future maritime platform.

The output section provides the robustness (fragmentation threshold) and communication efficiency versus the size of the giant component[29] (discussed in section 2.8) that is plotted, which shows the system's response to random failures. Finally, the hypotheses are tested by performing a statistical analysis of the experimental results using Minitab 18 software. The following sections provide a more detailed explanation of the resilience analysis framework.

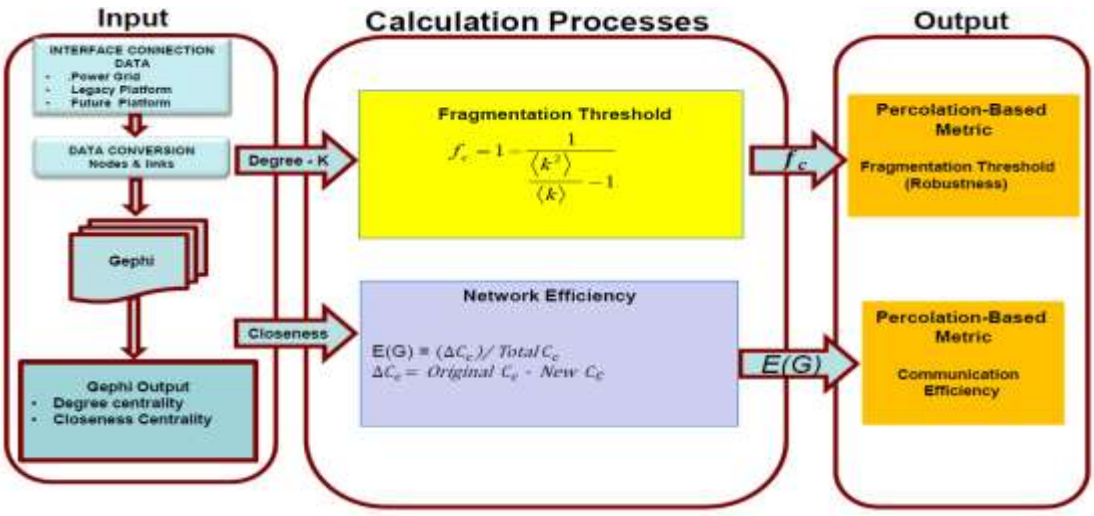

Figure 3-1: Percolation-based metric framework

[29] Giant component: a collection of connected nodes in which there is a path from each of the nodes.

3.2 Percolation Threshold

This praxis leveraged the work of Cohen et al. and Barabasi on percolation threshold phenomena to determine the resilience of maritime platforms (Cohen, 2003; Barabasi, 2016). As shown in Figure 3-2, a network is exposed to random breakdown when a fraction f of the total nodes and links fails randomly, causing the system integrity to be compromised; when f exceeds the percolation threshold $f > fc$, the network fragments into smaller and separated nodal elements. When f < fc, a connected spanning cluster or giant component exists with a size that is proportionate to that of the entire network. The fragmentation threshold f_c is the concentration f at which the state changes from one to zero, that is, from with connectivity to without connectivity. The failure of a single node or component has limited influence on the network's integrity. However, the failure of several nodes due to cascading failure[30] can break down the network into several components.

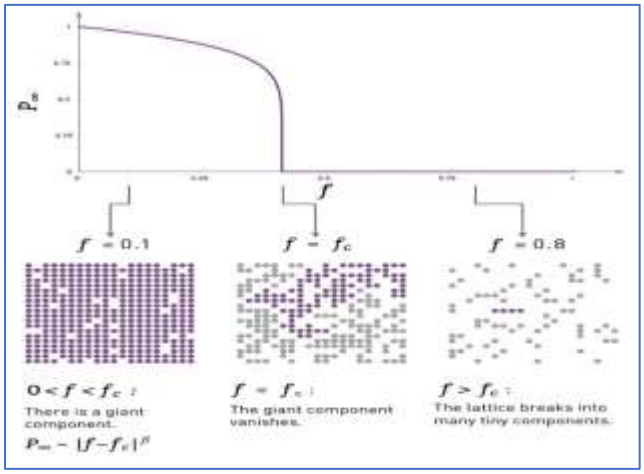

Figure 3-2: Percolation threshold (Barabasi, 2016; Image 8-4)

[30] Cascading failure: a process in a system of interdependent elements in which the failure of one element can trigger the failure of other elements (i.e., power grid, Internet, banking, transport, and roads).

3.3 Data Set, Collection, and Preparation Process

Figure 3-3 shows an example of the maritime platform's "Combat System Functional Diagram Summary" obtained from the functional interface requirement document, a document which defines the functional interfaces between all maritime systems, the integration of all subsystems, and the functions that support the missions of the maritime platform. Some examples of functional groupings are surveillance systems, shipboard control systems, mission control systems, weapon systems, navigation systems, communications systems, and support systems.

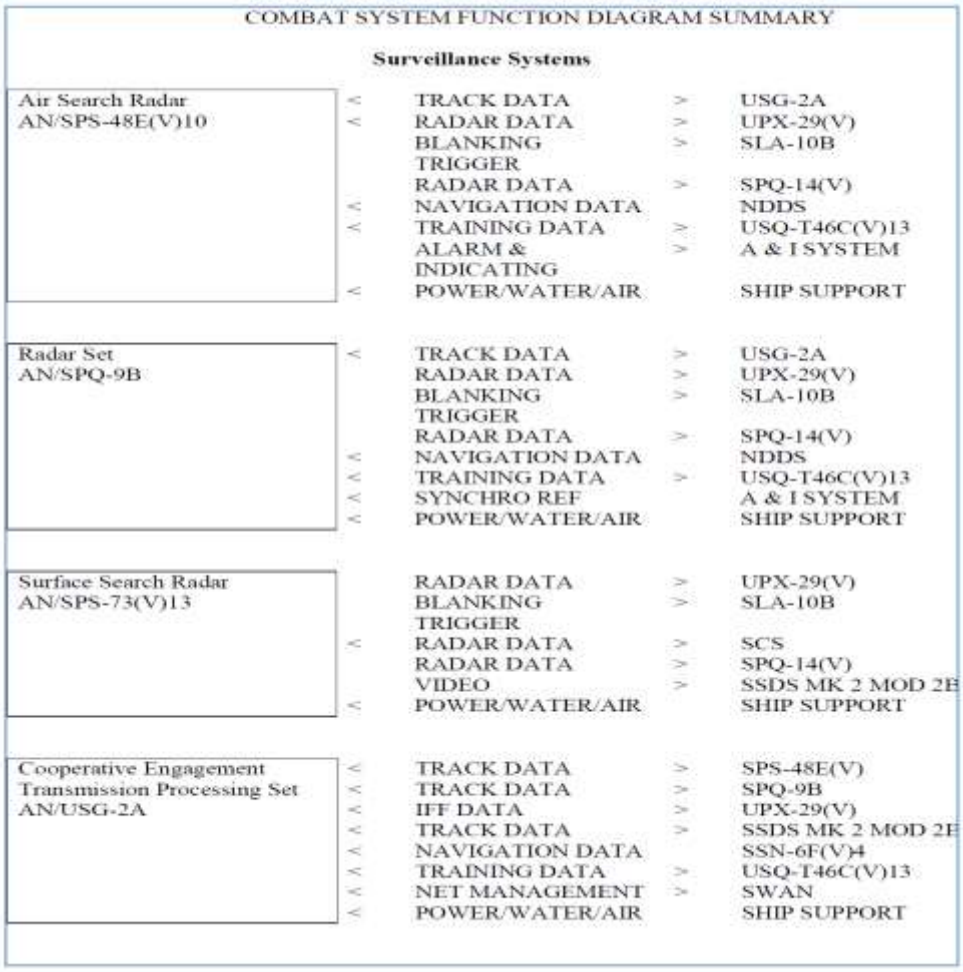

COMBAT SYSTEM FUNCTION DIAGRAM SUMMARY

Surveillance Systems

Air Search Radar AN/SPS-48E(V)10	<	TRACK DATA	>	USG-2A
	<	RADAR DATA	>	UPX-29(V)
		BLANKING TRIGGER	>	SLA-10B
		RADAR DATA	>	SPQ-14(V)
	<	NAVIGATION DATA		NDDS
	<	TRAINING DATA	>	USQ-T46C(V)13
		ALARM & INDICATING	>	A & I SYSTEM
	<	POWER/WATER/AIR		SHIP SUPPORT
Radar Set AN/SPQ-9B	<	TRACK DATA	>	USG-2A
		RADAR DATA	>	UPX-29(V)
		BLANKING TRIGGER	>	SLA-10B
		RADAR DATA	>	SPQ-14(V)
	<	NAVIGATION DATA		NDDS
	<	TRAINING DATA	>	USQ-T46C(V)13
	<	SYNCHRO REF		A & I SYSTEM
	<	POWER/WATER/AIR		SHIP SUPPORT
Surface Search Radar AN/SPS-73(V)13		RADAR DATA	>	UPX-29(V)
		BLANKING TRIGGER	>	SLA-10B
	<	RADAR DATA	>	SCS
		RADAR DATA	>	SPQ-14(V)
		VIDEO	>	SSDS MK 2 MOD 2E
	<	POWER/WATER/AIR		SHIP SUPPORT
Cooperative Engagement Transmission Processing Set AN/USG-2A	<	TRACK DATA	>	SPS-48E(V)
	<	TRACK DATA	>	SPQ-9B
	<	IFF DATA	>	UPX-29(V)
	<	TRACK DATA	>	SSDS MK 2 MOD 2E
	<	NAVIGATION DATA		SSN-6F(V)4
	<	TRAINING DATA	>	USQ-T46C(V)13
	<	NET MANAGEMENT	>	SWAN
	<	POWER/WATER/AIR		SHIP SUPPORT

Figure 3-3: Sample dataset (from FIRD)

Step 1, “Raw Data” (Figure 3-4), shows that the raw data sets come from two maritime platform FIRDs (legacy and future versions) and the power grid. The legacy and future platforms were built by the same shipbuilder (NAVSEA, 2001), and the Italian power grid data comes from ENTSOE (ENTSOE, 2017). The legacy platform was built in mid - 1990s, while the future platform was recently delivered to the navy. In Step 2, “Raw Data Conversion,” the functional interfaces are converted to nodes (equipment signals) and links (connection between equipment and systems) and formatted as CSV spreadsheet files for the Gephi software required format. In Step 3, “Data Import,” the nodes and links CSV file is imported into the Gephi software, then in Step 4, “Data Export from Gephi Software,” the centrality measures, system parameters, and network topology are extracted for further analysis.

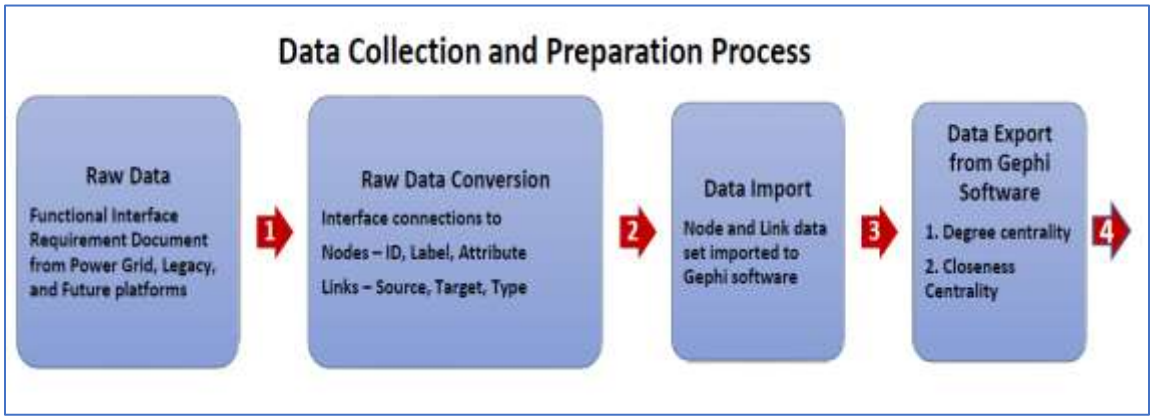

Figure 3-4: Data collection and preparation

The Gephi visualization software provides the centrality measures such as degree-k, closeness, betweenness, modularity, PageRank, clustering, Eigenvalue, and real-time topological display of the network. The software has the computational capability to accommodate a network with 20,000 nodes or more and can run several algorithms

simultaneously in separate workspaces. The output data is exportable in a CSV format. We only use the degree-k and closeness centrality information to calculate the fragmentation threshold and network communication efficiency, as shown in Step 4.

3.4 Method for Calculating Communication System Robustness

The primary focus of this praxis is robustness because this is the only resilience attribute that is quantifiable when component and system failure data are not available. Percolation theory can describe the impact of node failures on the integrity of the communication system's robustness (Karrer, 2014). Currently, no known publication concerning maritime communication systems that measure robustness using percolation theory. Since there are similarities between the maritime system and a power grid; power grid robustness is used as a baseline for comparison to complex and interdependent maritime platforms. Additionally, published datasets for the Italian power grids (Sole, 2007 Table 1; ENTSOE, 2017) were obtained to support the model validation and use as a baseline with which to compare the system fragmentation threshold.[31]

In Step 5 (Figure 3-6), the ID and degree-k data are extracted from the Gephi output and entered into the Excel spreadsheet (see Figure 3-5) to calculate the degree distribution (p_k) and fragmentation threshold (f_c). The degree distribution ($p_k = \frac{N_k}{N}$) denotes the probability that an arbitrarily chosen node has degree-k. The node degree (k) provides an insight into the structure of the network. Additionally, the degree-k distribution pinpoints the clusters or hubs that are formed within the network and

[31] The term fragmentation threshold is used in the context of this praxis to denote the breakup of the system from a functional to a nonfunctional network.

determines the system's vulnerability to cascading failures. The term N_k represents the network total nodes with a degree-k. Plotting p_k against k reveals the nodal distribution of the network, examples of destributions including Poisson, Gaussian, Exponential, or Power Law (scale-free) distributions (Estrada, 2012). In the context of this praxis, fragmentation threshold (f_c) terminology is used because the system robustness is computed by randomly fragmenting each node from a functional to a non-functional system. Percolation theory is applied, resulting in the random removal of each node to determine the robustness of the entire systems, namely, the legacy, future, and power grid networks. Using Equation (2-27) in Step 5, "Resilience Model," the average-k ($<k>$), variance-k ($<k^2>$), and fragmentation threshold (f_c) are calculated for each node (f_{cL} for legacy, f_{cF} for future, and f_{cPGI} for Italian power grid). Subsequently, in Step 6, "Fragmentation Plot," the nodal fragmentation threshold is plotted against the size of the giant component, averagef_c is computed, and a normality test is performed. In Step 7, the hypothesis test is performed using a statistical analysis of the experimental results.

ID	Degree <k>	pk =Nk/N	Rank	Average (Undirected) <k>	Average (Directed) <k>	Variance <k2>	Standard Deviation	fc
				8.58	4.29	1061.66	32.58	0.991855
760	3	0.000447	10	8.58	4.29	1062.97	32.60	0.991858
662	9	0.00134	10	8.58	4.29	1064.34	32.62	0.991869
629	4	0.000596	10	8.59	4.29	1065.67	32.64	0.991874
498	1	0.000149	10	8.60	4.30	1066.97	32.66	0.991875
666	1	0.000149	10	8.61	4.30	1068.26	32.68	0.991875
482	1	0.000149	10	8.62	4.31	1069.56	32.70	0.991876
686	4	0.000596	10	8.63	4.31	1070.91	32.72	0.991881
304	124	0.018463	10	8.48	4.24	1055.10	32.48	0.991901
611	1	0.000149	10	8.49	4.24	1056.39	32.50	0.991902
665	2	0.000298	10	8.49	4.25	1057.70	32.52	0.991904
720	2	0.000298	10	8.50	4.25	1059.02	32.54	0.991906
730	2	0.000298	10	8.51	4.26	1060.34	32.56	0.991908

Figure 3-5: Sample excel spreadsheet layout for robustness calculations
Note: Smaller fragmentation [value between 0 and 1] means that the system is less robust. While large fragmentation value means that the system is more robust.

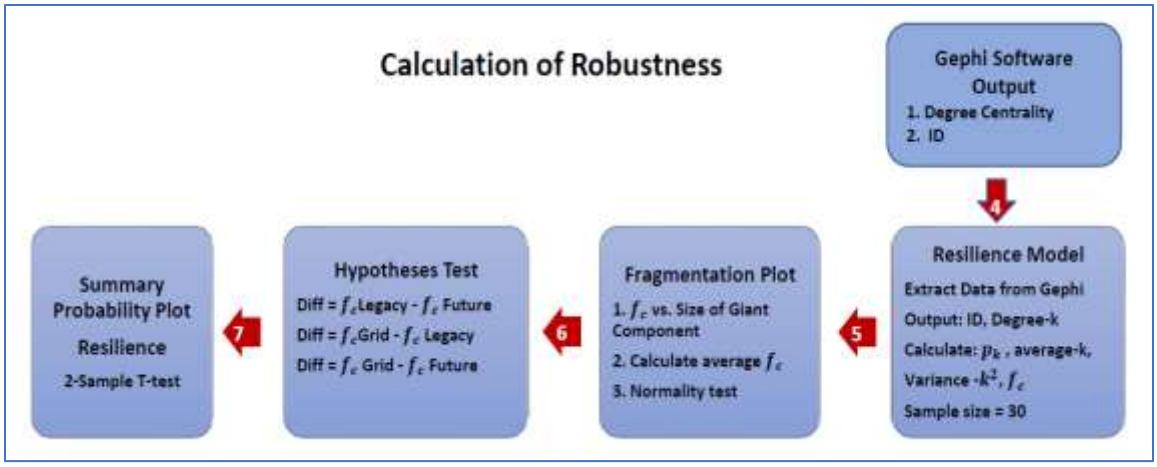

Figure 3-6: Calculation of robustness (fragmentation threshold)

3.5 Method for Calculating Communication System Efficiency

The functional interface requirement document (FIRD) can be used to model the communication system's efficiency. In this praxis, a social network analysis (SNA) technique is applied to measure the communication flow between the components or systems (nodes) and the system dependencies when random failures occur. The identification of the most critical node is quantified by centrality measures such as degree centrality, closeness centrality, or betweenness centrality. The capacity of a node to interconnect with and its distance from several other nodes determines the network's structural and functional properties. The degree to which the node is centralized affects its communication efficiency. In this praxis, two centrality measures are required to compute the network efficiency ($E(G)$).

In Step 4, "Gephi Software Output," (Figure 3-7), the first centrality measure is the degree centrality *(C_D)*, which accounts for the total links *(L)* that communicate with a node *(N)*. The amount of C_D is proportional to the node degree and it models the

communication flow between the network nodes (Estrada, 2012, p. 123). In a directed network, there are two types of degree centrality, namely in-degree as the incoming connection and out-degree as the outgoing connection of a node (Estrada, 2012, p. 123). The degree centrality C_D of a node N is as follows:

$$C_D(N) = \text{degree-k (N)} = \text{(In-degree)} + \text{(Out- degree)} \quad (3\text{-}1)$$

The second centrality measure is the closeness centrality (C_C), which specifies the time required for information to flow from a node m and reach the other node n in the network (Estrada, 2012, p. 140; Latora and Marchiori, 2007, p. 3). Closeness centrality measures the communication efficiency of a specific node within a network (Yen, Yeh, and Chen, 2013).

$$C_c = L^{-1} = \frac{N-1}{\sum_{n \epsilon G} d_{m,n}} \quad (3\text{-}2)$$

In Equation (3-2), the shortest path distance ($d_{m,n}$) represents the total links in the direct path connecting nodes m and n in a network. When there is no connection between two nodes, the distance between them is set to indefinite, $d\ (m, n) = \infty$. The average length of the shortest path (L^{-1}) quantifies the flow of information by taking the average of all the nodes that are part of a connection between a pair of nodes m and n (Estrada, 2012, p. 49). In Step 5, "Efficiency Model," the communication efficiency ($E(G)$) is measured by taking the change in the system efficiency of the communication flow when a node is removed from the entire network ΔC_C compared to the Total C_C; we thus define E(G):

$$E(G) = \frac{\Delta C_C}{Total\ C_C} \quad (3\text{-}3)$$

In Step 6, "Efficiency Plot," the communication efficiency is plotted against the size of the giant component, the average efficiency is computed, and a normality test is performed. In Step 7, a hypothesis test is performed via a statistical analysis of the experimental results using Minitab 18 software. Step 8, "Summary Probability Plot," presents the results of the normality test. Figure 3-8 displays the sample spreadsheet layout for network communication efficiency calculations.

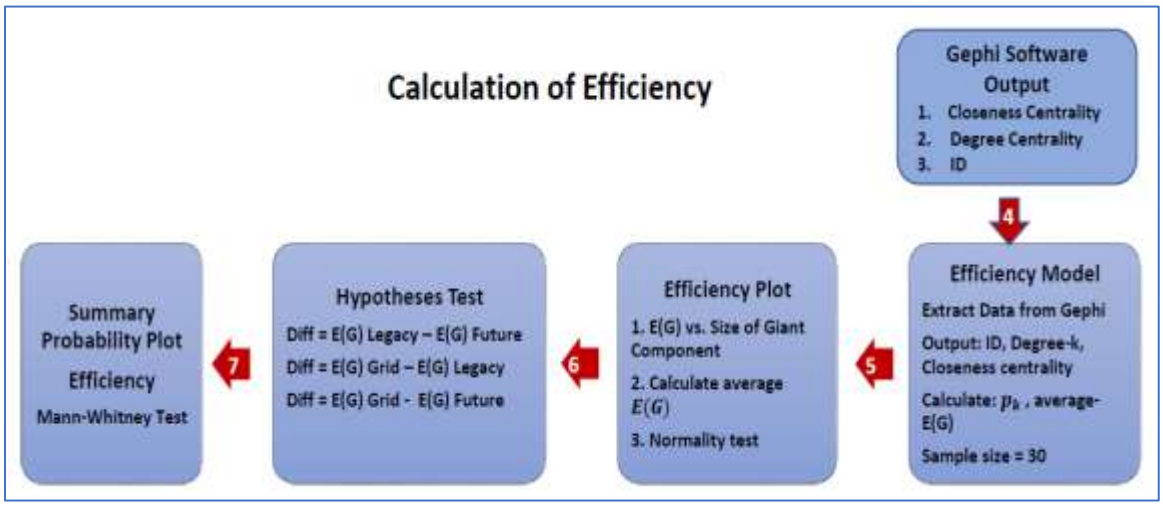

Figure 3-7: Calculation of communication efficiency

ID	Degree-k	pk=Nk/N	Rank	Network Size %	Closeness Centrality	Average Efficiency E(G)
				1		0.372470281
316	3	0.000457	10	0.999543	0.203370	0.372639891
580	8	0.001218	10	0.998325	0.142543	0.372870911
259A	1	0.000152	10	0.998172	0.169216	0.37307559
551	3	0.000457	10	0.997716	0.000000	0.373450917
385	4	0.000609	10	0.997106	1.000000	0.372819951
110	2	0.000305	10	0.996802	1.000000	0.372187714
909	0	0	10	0.996802	0.000000	0.372563281
799	3	0.000457	10	0.996345	0.220851	0.372716526
277	2	0.000305	10	0.99604	0.166081	0.37292546
875	0	0	10	0.99604	0.000000	0.373302915
584	13	0.00198	10	0.99406	0.191725	0.373486884
102	2	0.000305	10	0.993756	1.000000	0.372851475

Figure 3-8: Sample excel spreadsheet layout for communication efficiency calculations

3.6 Statistical Test

For samples with normal distributions, the 2-Sample T-Test with a 95% confidence interval is applied to determine whether the population means of two independent groups differ (Minitab 2018). For a sample with non-normal distribution, a non-parametric test (Mann-Whitney) is applied to determine whether the population medians of two independent groups differ (Minitab 2018). A sample size $n \geq 30$ is chosen to ensure that the sampling distribution is approximately normal. Thus, the test statistics are based on normal z-statistics.

3.7 Summary

A percolation-based metric framework is developed to measure the robustness and efficiency of the communication system. Using this framework, the raw data from the maritime platform FIRD is transformed into node (N) and link (L) format for the Gephi

SNA software, which provides the centrality measure parameters required to compute robustness (fragmentation threshold) and efficiency of the communication system. By randomly fragmenting the nodes, the communication system's robustness and efficiency are measured and plotted for analysis. The next section presents the detailed results of the experiments using two power grids and two maritime platforms.

Chapter 4: Results

This chapter provides the results of the research and answers to the primary research questions. Example output data is first presented, followed by robustness (fragmentation threshold) and efficiency results along with graphical plots of the system response. Finally, the statistical test results are shown with summary plots.

4.1 FIRD Conversion

Figure 4-1 presents an example of the Gephi software output. The nodes and links raw dataset obtained from the FIRDs is abstracted and imported into the SNA (Gephi).

ID	In Degree	Out Degree	Degree Centrality	Closeness Centrality	Betweeness Centrality	PageRanks	Strong component	Clustering	Eigen centrality
0	0	0	0	0	0	1.94E-04	0	0	0
1	0	11	11	0.231496063	0	1.94E-04	325	0	0
2	1	72	73	0.207850708	1.55E-04	2.09E-04	324	0	2.88E-04
3	1	16	17	0.191435768	6.01E-05	2.09E-04	252	0	2.88E-04
4	1	13	14	0.179714091	2.57E-05	2.09E-04	239	0.06043956	2.88E-04
5	1	17	18	0.214054927	8.35E-05	2.09E-04	230	0.00980392	2.88E-04
6	1	15	16	0.198201574	6.16E-05	2.09E-04	219	0	2.88E-04
7	1	6	7	0.175616346	6.94E-05	2.09E-04	209	0	2.88E-04
8	1	23	24	0.210772834	2.04E-04	2.09E-04	208	0	2.88E-04
9	1	2	3	0.75	3.02E-06	2.09E-04	187	0	2.88E-04
10	1	2	3	0.105146317	3.17E-05	2.09E-04	184	0	2.88E-04
11	1	5	6	0.363636364	1.16E-05	2.09E-04	30	0	2.88E-04
12	1	16	17	0.490566038	2.16E-05	2.09E-04	22	0	2.88E-04
13	0	3	3	0.133283133	0	1.94E-04	337	0	0
14	1	8	9	0.146625937	4.54E-04	2.49E-04	336	0	2.88E-04
15	1	1	2	0.11547857	3.78E-05	2.49E-04	327	0	2.88E-04
16	1	1	2	0.11578713	3.88E-05	2.49E-04	326	0	2.88E-04
17	0	5	5	0.176764314	0	1.94E-04	349	0	0
18	1	3	4	0.19847619	2.95E-04	2.27E-04	348	0	2.88E-04
19	1	2	3	0.17339113	9.49E-06	2.27E-04	346	0	2.88E-04
20	1	6	7	0.199004975	1.98E-04	2.27E-04	345	0	2.88E-04
21	1	4	5	0.143288498	4.52E-06	2.27E-04	344	0	2.88E-04
22	1	4	5	0.1886044	2.11E-05	2.27E-04	341	0.15000001	2.88E-04
23	0	9	9	0.223468162	0	1.94E-04	384	0	0
24	1	9	10	0.197652404	1.18E-05	2.12E-04	383	0.02222222	2.88E-04
25	1	10	11	0.250120019	3.40E-04	2.12E-04	380	0	2.88E-04
26	1	5	6	0.187410587	1.21E-05	2.12E-04	378	0	2.88E-04
27	1	36	37	0.196200219	6.94E-05	2.12E-04	373	0	2.88E-04
28	1	6	7	0.19138756	9.27E-05	2.12E-04	355	0	2.88E-04

Figure 4-1: Sample Gephi output showing centrality measures

4.2 Degree Centrality Distribution Test

The degree centrality represents the total number of links connected to other nodes and describes the importance of the node. In Figure 4-2, we plotted and compared the degree-k distribution for the Italian power grid and the legacy and future platforms to determine the distribution of the systems under study. Figure 4-2 (a & b) shows the exponential distribution of the Western and Italian power grid data, while Figure 4-2 (c & d) shows the scale-free distribution of the legacy and future shipboard platforms.

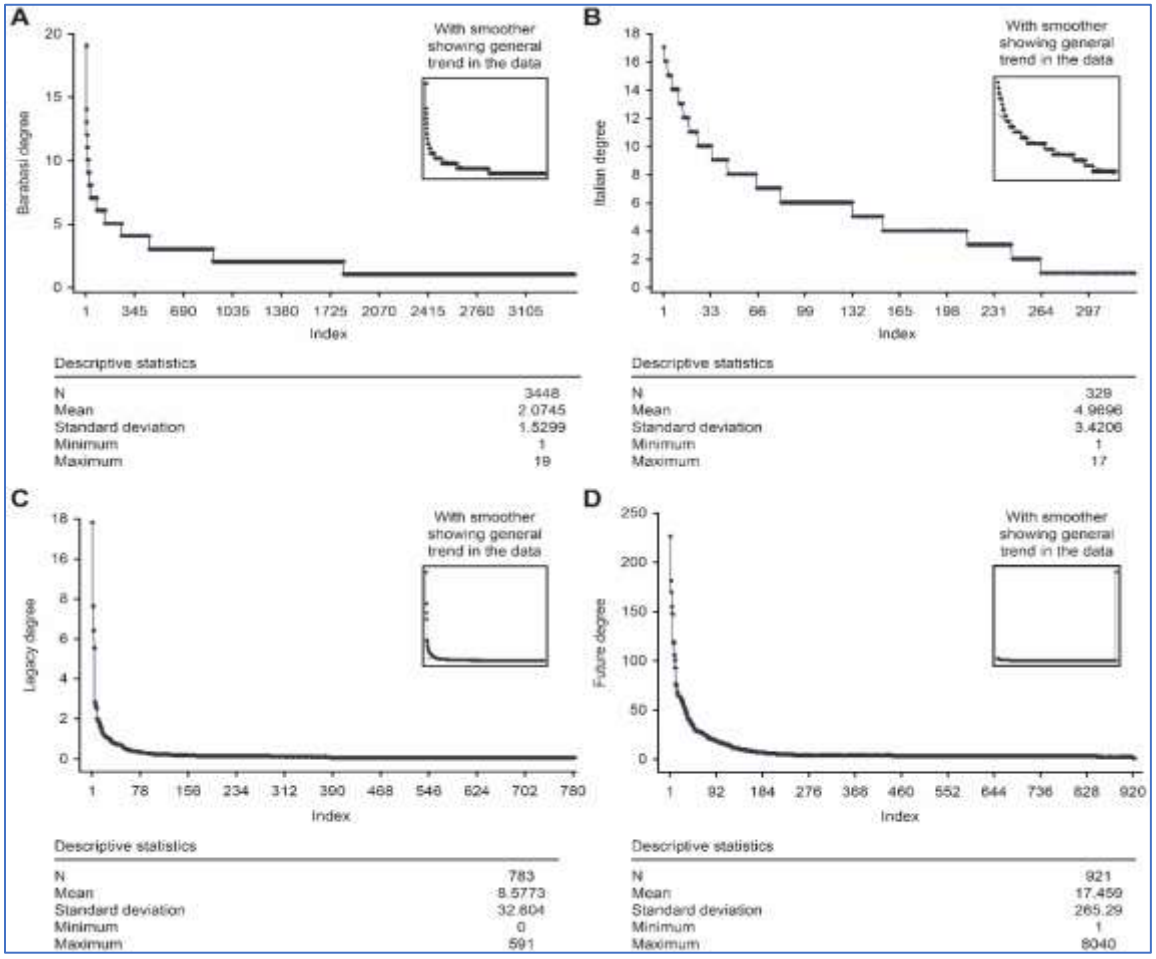

Figure 4-2: Degree centrality distribution plots

4.3 Fragmentation Threshold Simulation Results

The nodal fragmentation is performed by removing each node using Equation (2-27). Table 4-1 presents this process in a spreadsheet format for the power grid and the legacy and future maritime platforms. The random removal of the nodes is simulated 30 times for each population, and the results of the fragmentation experiment are presented in Table 4-1.

Table 4-1: Calculated metric data for fragmentation threshold (fc)

Sample	1	2	3	4	5	6	7	8	9	10	11	12	13	14	15
Fragmentation Threshold Italian Pwr Grid (Fc)	0.336922	0.527565	0,297766	0.200479	0.32951	0.281852	0.332186	0.300314	0.329892	0.209819	0.411347	0.30463	0.383386	0.222985	0.254473
Fragmentation Threshold Legacy platform (Fc)	0.975296	0.985477	0.991528	0.977102	0.985485	0.988131	0.970504	0.970509	0.990118	0.990506	0.983765	0.982427	0.966207	0.966207	0.960047
Fragmentation Threshold Future platform (Fc)	0.954233	0.972092	0.971043	0.967587	0.973536	0.967898	0.971369	0.962914	0,961269	0.970289	0.95609	0.93361	0.980213	0.963044	0.970328
Sample	16	17	18	19	20	21	22	23	24	25	26	27	28	29	30
Fragmentation Threshold Italian Pwr Grid (Fc)	0.246304	0.336087	0.311577	0.229367	0.193798	0.326037	0.438484	0.211494	0.305009	0.29422	0.303531	0.291285	0.39068	0.245341	0.194131
Fragmentation Threshold Legacy platform (Fc)	0.993565	0.978306	0.966099	0.979774	0.983601	0.989178	0.989905	0.975623	0.963875	0.964682	0.987553	0.976076	0.991692	0.980107	0.987093
Fragmentation Threshold Future platform (Fc)	0.975704	0.960422	0.963494	0.965172	0,971433	0.978933	0.955461	0.968196	0.960821	0.960821	0.97963	0.966969	0.959753	0.963741	0.968727

The percolation-based metric framework shown in Figure 3-1 and Figure 3-6 are followed to compute the robustness (fragmentation threshold). The next step is to determine whether the data follow a normal distribution by comparing the *p-value* to the significance level (α = 0.05) using the Anderson-Darling Test (Minitab 8.0). If the *p-value is* $\leq$ *0.05*, then the data do not follow a normal distribution, thus rejecting the null hypothesis H_o. If the *p-value is > 0.05*, then we cannot conclude that the data fail to follow a normal distribution, thus failing to reject H_o.

Null hypothesis H_o : *Data follows a normal distribution*

Alternative hypothesis H_1 : *Data do not follow a normal distribution*

Figure 4-3 shows the results of the probability plot, with the Anderson-Darling Test indicating *p-values > 0.05* (inside the red box), meaning that the samples have a normal distribution. Thus, the 2-Sample T-Test is appropriate to compare the means of the populations under study.

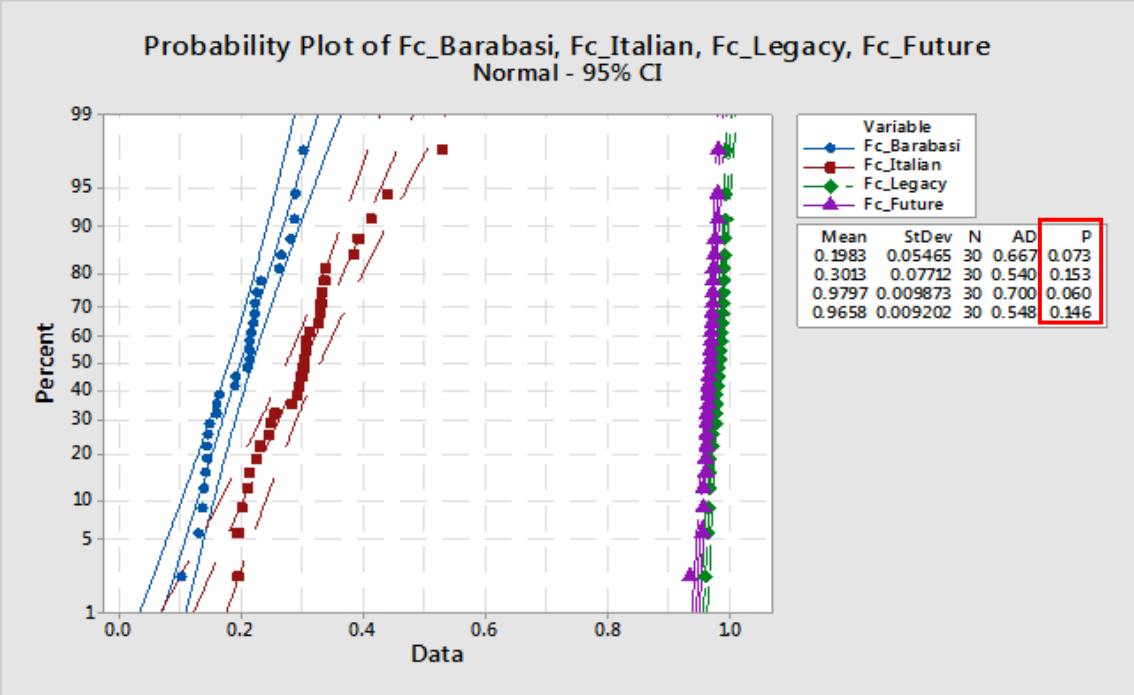

Figure 4-3: The probability plot corresponds to the summary results of our experiment using N = 30 samples. The plot of the means for the Barabasi = 0.1983, Italian power grid = 0.3013, legacy =0.9797, and future = 0.9658.

In Step 6 (Figure 3-6), the fragmentation threshold is plotted against the size of the giant component to determine the communication system's response when nodes are removed randomly. The figures 4-4 through 4-6 present six sample plots of the robustness (fragmentation threshold) versus the size of the giant component. The Italian power grid's best system response to the random removal of nodes is shown in (a) through (c), depicting minimal fragmentation with f_{cPGI} equal to 0.86, 0.68, and 0.63, while (d) through (f) show

the fast fragmentation with f_{cPGI} equal to 0.58, 0.52, and 0.33, even during the random removal of nodes. The legacy maritime platform's best system response to the random removal of nodes is shown in (a) through (c), depicting negligible fragmentation with f_{cL} equal to 0.999, 0.995, 0.992, while (d) through (f) show the slow fragmentation of the communication system at approximately 99% node removal with f_{cL} equal to 0.993, 0.996, and 0.994. The future maritime platform's best system response to the random removal of nodes is shown in (a) through (c), depicting negligible fragmentation with f_{cF} with 0.989, 0.982, and 0.992, while (d) through (f) show the slow fragmentation of the communication system at approximately 99% node removal with f_{cF} equal to 0.975, 0.997, and 0.977.

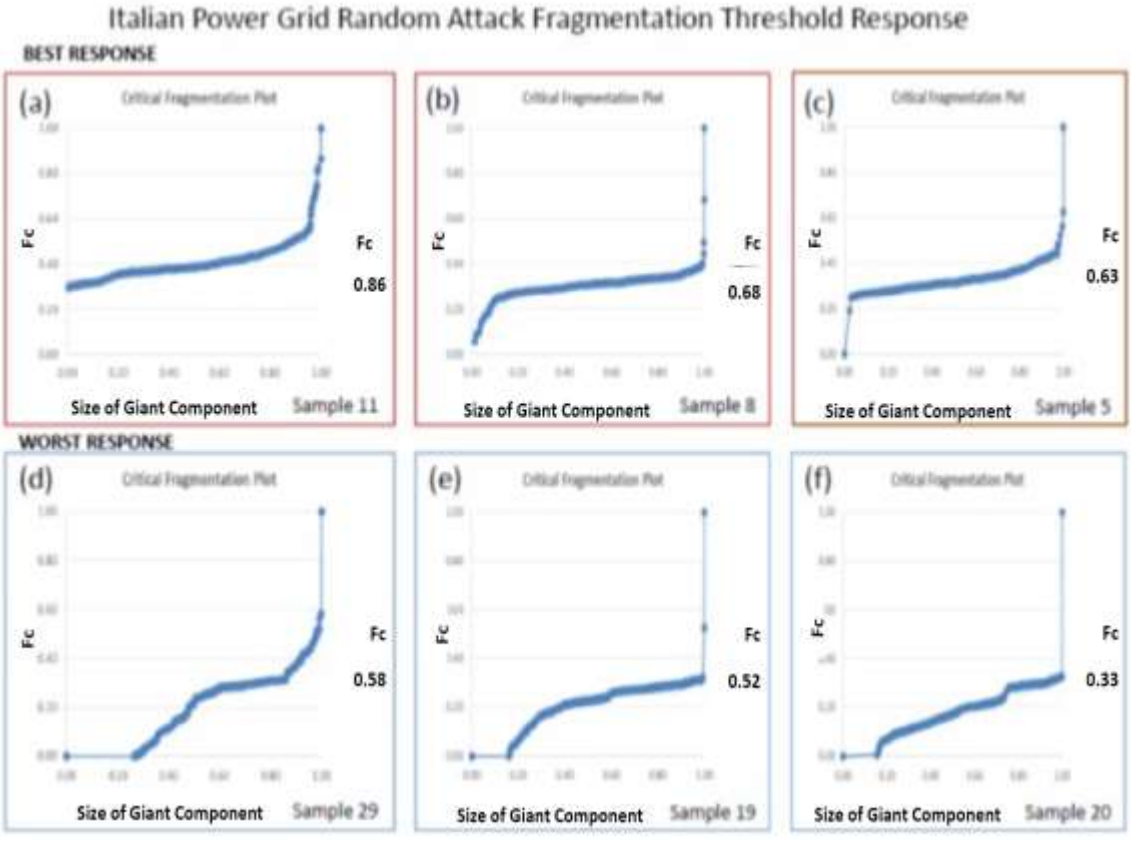

Figure 4-4: Network robustness measure for the Italian power grid data using the inverse percolation method with N = 329 and total degree-k = 1624 connections.

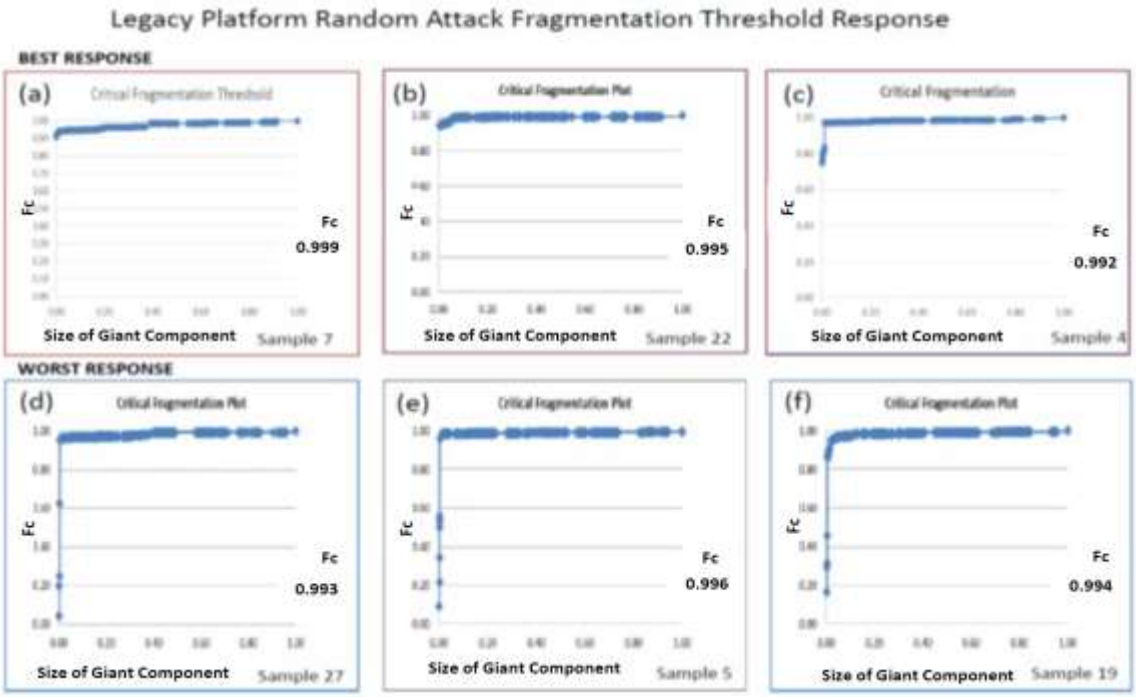

Figure 4-5: Network robustness measure for the legacy platform data using the inverse percolation method with N = 782 and total degree-k = 6716 connections.

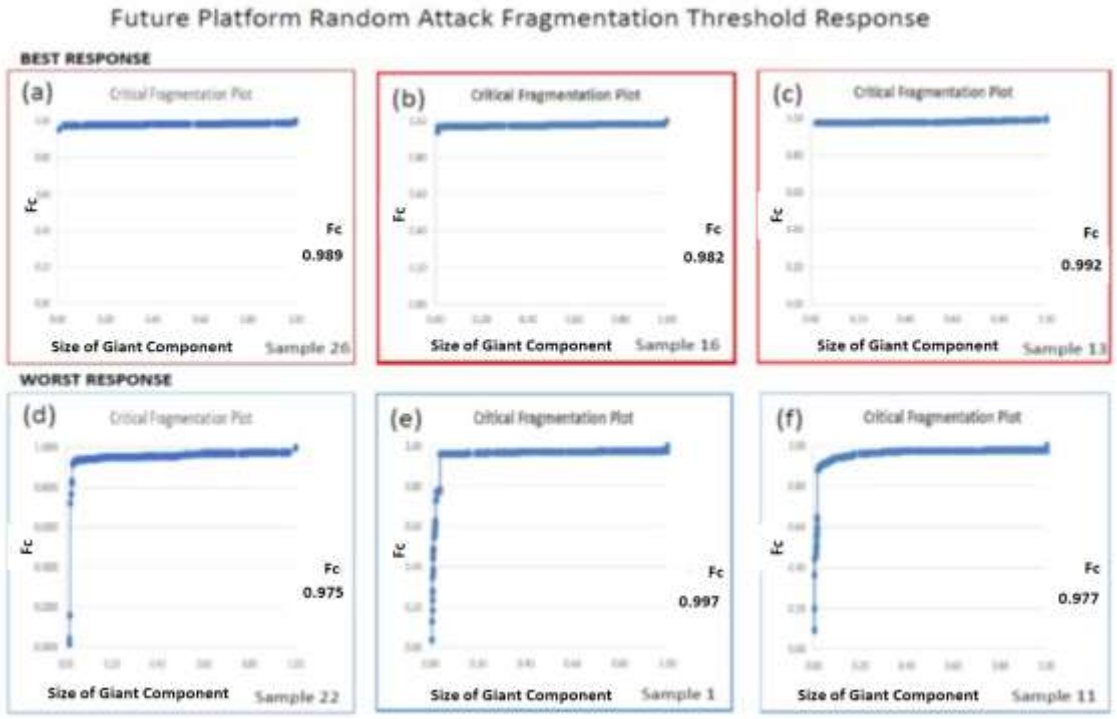

Figure 4-6: Network robustness measure for the future platform data using the inverse percolation method with N = 920 and total degree-k = 8040 connections.

Table 4-2 shows the summary of the robustness (fragmentation threshold) hypothesis test using the 2-Sample T-Test. The Hypotheses 3a, 4a1, and 4b1 are tested with a *p-value of* ≤ 0.05.

Table 4-2: Summary hypothesis test for robustness (fragmentation threshold) [2-Sample T-test]

System	Number of Samples	Mean	95% Confidence Interval	Standard Deviation	P-value
Hypothesis 3a Difference = Fc legacy – Fc future = + 0.013855					
legacy	30	0.97968	0.9760, 0.9834	0.0098734	P < 0.001
future	30	0.96583	0.96239, 0.96926	0.0092023	
Hypothesis 4a1 Difference = Fc Pwr Grid – Fc legacy = -0.67833					
Pwr Grid	30	0.30135	0.2774, 0.3253	0.0771220	P < 0.001
legacy	30	0.97968	0.97662, 0.98274	0.0098734	
Hypothesis 4b1 Difference = Fc Pwr Grid – Fc future = -0.066448					
Pwr Grid	30	0.30135	0.2774, 0.3253	0.077122	P < 0.001
future	30	0.96583	0.96297, 0.96868	0.0092023	

4.4 Communication Efficiency Simulation Results.

The communication efficiency is measured by removing each node using Equation (3-3), the processes outlined in Figure 3-7 process, and the spreadsheet format presented in Figure 3-8. The data is presented in Table 4-3.

Table 4-3: Calculated metric data for communication Efficiency, *E (G)*

Sample	1	2	3	4	5	6	7	8	9	10	11	12	13	14	15
Power Grid Network Communication Efficiency E(G)	0.117630	0.113861	0.115491	0.121489	0.117894	0.139157	0.122991	0.121288	0.121951	0.116969	0.120851	0.119537	0.120905	0.121890	0.129948
Legacy Network Communication Efficiency E(G)	0.102297	0.114193	0.118869	0.117674	0.111057	0.116058	0.111755	0.111608	0.107269	0.100558	0.112599	0.112841	0.107822	0.107451	0.129685
Future Network Communication Efficiency E(G)	0.974184	0.977740	0.978411	0.974827	0.973517	0.973020	0.974919	0.974670	0.975805	0.977652	0.979508	0.980735	0.976617	0.979663	0.978985
Sample	16	17	18	19	20	21	22	23	24	25	26	27	28	19	30
Power Grid Network Communication Efficiency E(G)	0.122719	0.116968	0.116019	0.124546	0.122305	0.001177	0.118148	0.113158	0.115724	0.132106	0.119068	0.101499	0.116243	0.120119	0.121781
Legacy Network Communication Efficiency E(G)	0.107742	0.115370	0.103263	0.109153	0.106996	0.106736	0.106785	0.106257	0.129685	0.107556	0.110047	0.104829	0.119739	0.116126	0.120817
Future Network Communication Efficiency E(G)	0.976703	0.977451	0.976475	0.976370	0.976528	0.979057	0.981264	0.979038	0.976154	0.979344	0.977736	0.975602	0.976354	0.975154	0.976154

The communication efficiency is directly proportional to the closeness centrality measure. A nodal fragmentation is performed by removing each node using Equation (2-27) and calculating the communication efficiency using Equation (3-3). The nodal fragmentation shows the effect of closeness centrality on communication efficiency and the effect of degree-k on the size of the giant component, The communication efficiency *(E(G))* and the size of the spanning cluster are dependent on the removal of nodes with degree-k connections. The figure 4-10 shows the Anderson-Darling test for normality, with p-values that are less than 0.05. We can conclude that the data fail to follow a normal distribution, failing to reject $H_{o.}$ Since the data have a non normal distribution, a non-parametric test such as the Mann-Whitney test is

appropriate. Table 4-5 presents the summary of the communication efficiency hypotheses test using the Mann-Whitney test.

In Table 4-4, Hypothesis # 3b, since the *p-value* $\leq$ *0.05*, the difference between the median is statistically significant, therefore reject H_o at a 95% confidence interval. The future maritime platform communication efficiency median (E_{GF} = 0.97665) is significantly different from that of the legacy maritime platform (E_{GL} = 0.10960). In Table 4-4, Hypothesis # 4a2, since the *p-value* $\leq$ *0.05*, the difference between the median is statistically significant, and therefore, we can reject H_o at a 95% confidence interval. The Italian power grid median (E_{GPI} = 0.119829) is significantly different than the legacy maritime platform (E_{GL} = 0.109600). In Table 4-4, Hypothesis # 4b2, since the *p-value* $\leq$ *0.05*, the difference between the median is statistically significant, and therefore, we can reject H_o at a 95% confidence interval. The Italian power grid median (E_{GPI} = 0.119828) is significantly different than the mean of the future maritime platform (E_{GF} = 0.97660).

The figures 4-7 through 4-9 present six sample plots of the Italian power grid, and the legacy and future maritime platform communication efficiency against the size of the giant component. For the Italian power grid, the best system response to random removal of nodes is shown in (a) through (c), depicting best communication efficiency, which was equal to 0.46, 0.38, 0.20; meanwhile, (d) through (f) display the worst communication efficiency, equal to 0.14, 0.13, 0.13 after the removal of nodes. For the legacy maritime platform, the best system response to random removal of nodes is shown in (a) through (c), depicting best communication efficiency, which is equal to 0.26, 0.25, 0.23; by contrast, (d) through (f) display the worst communication efficiency, which is

equal to 0.117, 0.118, 0.119 after the removal of nodes. For the future maritime platform, the best system response to the random removal of nodes is shown in (a) through (c), depicting best communication efficiency, which is equal to 0.93, 0.76, 0.77; (d) through (f), meanwhile, demonstrate the worst communication efficiency, equal to 0.38, 0.37, 0.40 after the removal of nodes. Figure 4-10 shows the summary probability plots of the Italian power grid and the legacy and future maritime platform's communication efficiency, showing *p-values < 0.05*.

Table 4-4: Summary hypothesis test for communication efficiency (Mann-Whitney test)

System	Number of Samples	Median	95% Confidence Interval	Achieved Confidence	P-value
Hypothesis 3b Difference = E(G) legacy — E(G) future = - 0.867307					
legacy	30	.10960	-0.869345, -0.86461	95.16%	0.000
future	30	.97666			
Hypothesis 4a2 Difference = E(G) Pwr Grid — E(G) legacy = + 0.0092870					
Pwr Grid	30	0.119828	0.0063050, 0.0120860	95.16%	0.000
legacy	30	0.109600			
Hypothesis 4b2 Difference = E(G) Pwr Grid — E(G) future = - 0.857678					
Pwr Grid	30	0.119828	-0.859448, -0.855762	95.16	0.000
future	30	0.976660			

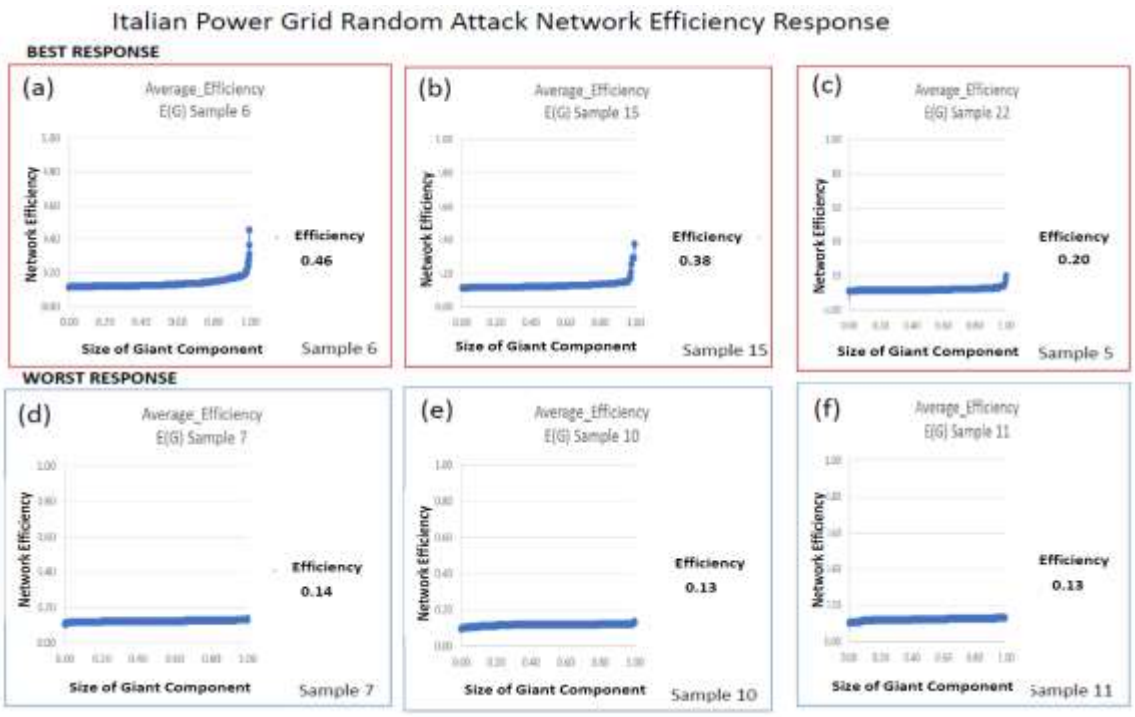

Figure 4-7: Communication efficiency measure for the Italian power grid using the inverse percolation method with N = 329 and total degree-k = 1624 connections.

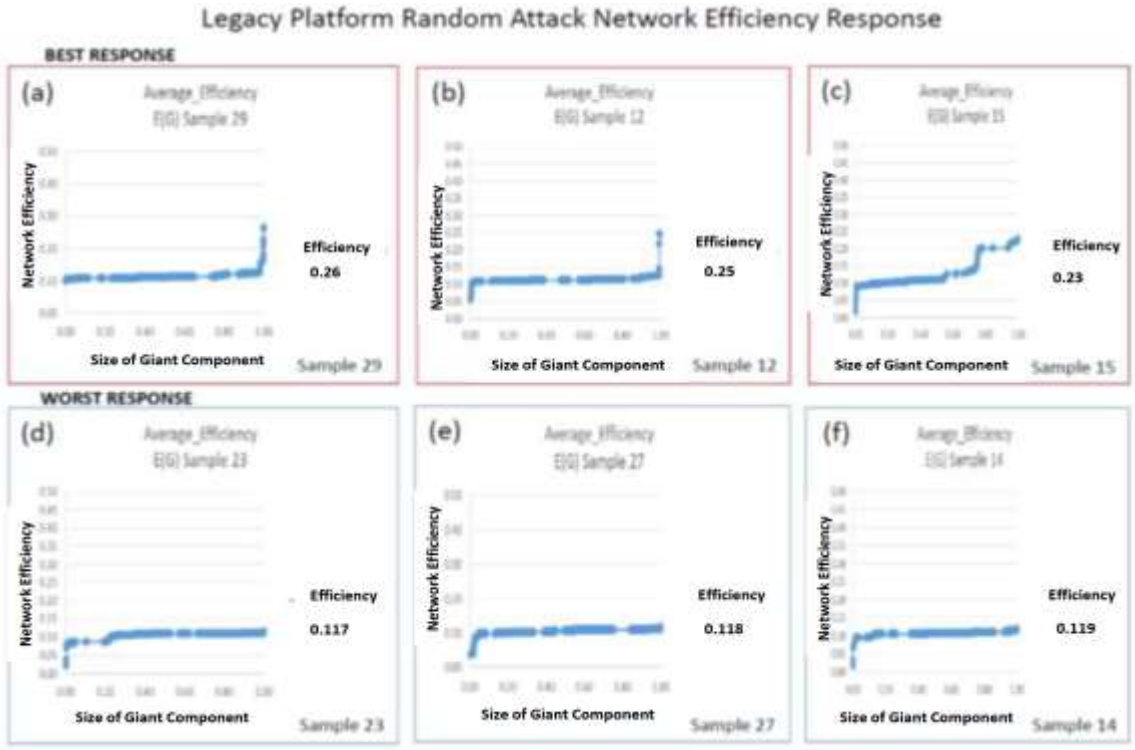

Figure 4-8: Communication efficiency measure for the legacy maritime platform using the inverse percolation method with N = 782 and total degree-k = 6716 connections.

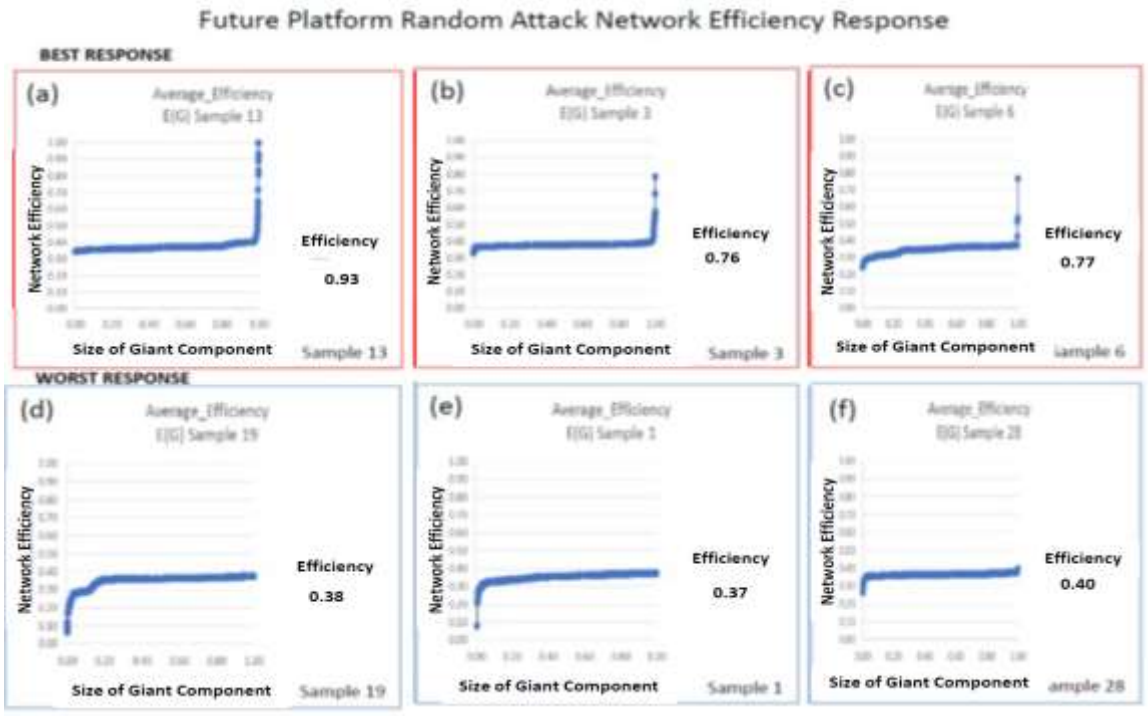

Figure 4-9: Communication efficiency measures for the future maritime platform using the inverse percolation method with N = 920 and total degree-k = 8040 connections.

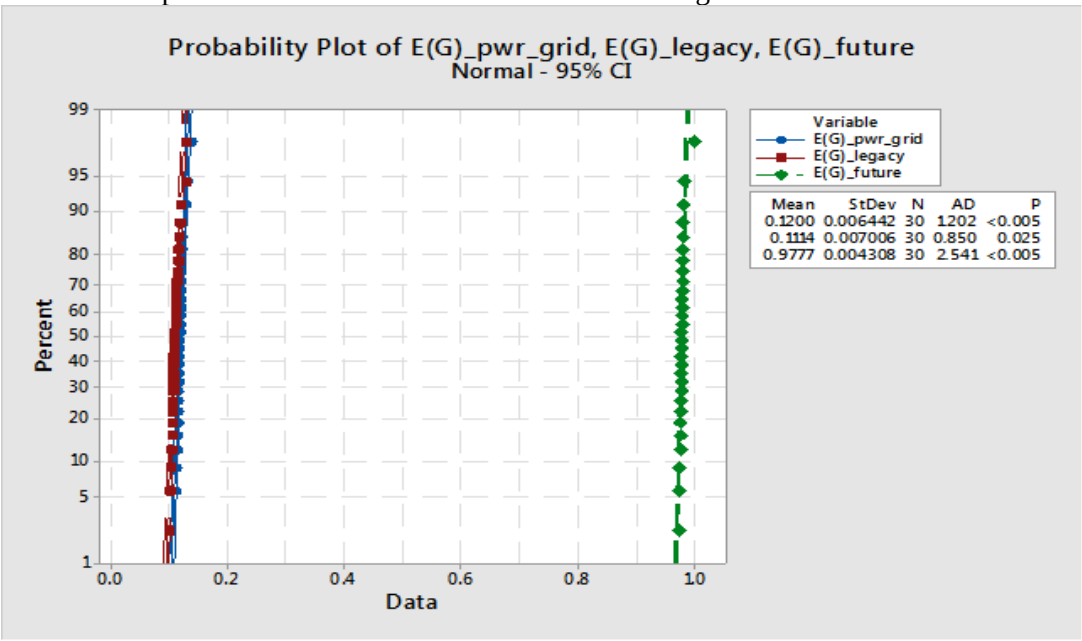

Figure 4-10: The probability plot results corresponding to the summary results of our experiment using N = 30 samples. The plot of the means for the Italian power grid = 0.1200, legacy = 0.1114, and future = 0.9777.

Chapter 5: Discussion and Conclusion

5.1 Discussion

The experimental results confirm that a percolation-based metric framework is a viable method for generating a rank order of system proposals. The percolation-based metric method is practical, can distinguish between four real networks such as the Western power grid, Italian power grid, legacy maritime platform, and future maritime platform, and can inform engineering decisions during the comparison of alternative proposals. This research identified and quantified two percolation-based metrics for communication systems, namely, robustness (larger fragmentation threshold (f_c)) and efficiency ($E(G)$), that are able to analyze complex, interdependent, and resilient systems.

Resilience theory plays a vital role in the practical design of modern communication systems composed of CPSs and components including interdependencies intended to make the entire system robust. However, there is no consistent and reliable metric (Uday, 2015) for resilience because resilience theory is approached from various viewpoints and defined differently across several domains (Bhamra, 2011; Hosseini, 2016). Thus, the quantitative methods through which system designers can analyze complex and resilient systems remain unclear and not fully defined. The literature research shows that quantitative measures are domain-dependent, and the quantitative methods that are available such as FTA, BN, and MC have limitations due to system complexity, dependencies, and system coupling (Vesely, 1981). The identification of specific quantitative method(s) capable of supporting complex and resilient systems will facilitate the development of robust, efficient, and cost-effective communication systems.

This praxis employs a percolation-based metric framework to model the failure of the communication system's components and systems by removing fractions of the nodes or links, rendering the functional networks non-functional. The percolation-based metric approach was applied to the Western and Italian power grids and the legacy and future maritime platforms to model system robustness (larger fragmentation threshold (f_c)) and efficiency ($E(G)$) of the communication systems. The percolation-based metric framework was applied due to its ability to model system interdependencies by using the maritime platform FIRDs without relying on reliability data; sample Gephi output is shown in Figure 1-3. The result of the experiments and statistical analysis are discussed below.

5.1.1 Nodal Distribution

The degree-k distribution values correspondingo the degree centrality which is plotted to determine the nodal distribution of the system. The figures 4-2 (a) and 4-2 (b) shows that the degree-k distribution for the Western and Italian power grids are exponential distributions which validate the initial study by Sole and others. The findings on the Italian power grid distribution replicate the outcomes noted by Sole et al. (Sole, 2007). Figure 4-2 (c & d), the legacy and future maritime platform degree-k show "fat-tail" or scale-free distribution. A fat-tail distribution is characterized by a smaller quantity of nodes with a high degree-k and a larger quantity of nodes with a lower degree-k. The significance of analyzing the degree-k distribution is the ability to identify clusters or hubs within the interdependent system that make the system susceptible to cascading failures (Zheng, 2007). Currently, there is no known degree-k distribution measure for maritime platforms, and this praxis provides the first degree-k measure.

5.1.2 Fragmentation Threshold Hypothesis Test

This section discusses the hypotheses tests. For Hypothesis 3a, we can conclude that the mean robustness (fragmentation threshold (f_{cL})) of the legacy maritime platform is significantly different from that of the future maritime platform at a 0.05 significance level, making the legacy's robustness (fragmentation threshold) more significant than that of the future. For Hypotheses 4a1 and 4b1, we can conclude that the mean robustness (fragmentation threshold (f_{cPGI})) of the Italian power grid is significantly less than that of the legacy and future maritime platforms at a 0.05 significance level. The initial assumption was that the maritime platform robustness (fragmentation threshold) is similar to that of the power grid. However, the outcome of this research shows that the legacy and future maritime platform robustness (fragmentation thresholds) are significantly greater than that of the power grid.

5.1.3 Comparison of Legacy and Future Maritime Platforms

Since both the legacy and future maritime platforms came from the same shipbuilder with the same design, one would assume that the future maritime platform design is more robust to nodal failure than the legacy maritime platform design, which originated earlier. However, the results of Hypothesis 3a demonstrate otherwise. The legacy maritime platform is more robust. Further analysis of the average degree–k and variance degree-k revealed that the future maritime platform has smaller variance due to nodes being clustered together, while the legacy maritime platform has considerable variance due to widely scattered nodes. The improvements in the future maritime platform design have resulted in a sparse network. For instance, the legacy maritime platform has 11 large hubs

with 90 to 591 degree-k connections, while the future maritime platform has six large hubs with 103 to 202 degree-k connections.

5.1.4 Significance of Experiments

The significance of the nodal fragmentation experiment is that the random removal of nodes with fewer connections (smaller degree-k) does not result in the breakdown of the entire communication system. However, the sequential removal of nodes with more prominent connections (hubs) or a larger degree-k gradually results in the breakdown of the communication system (see Figures 4-4 through 4-6). This praxis replicates the findings of random attacks on power grids (Wang, 2009) and the Internet (Barabasi, 2016). Thus, when a failure of a node or link occurs on an interdependent network, a cascading failure between the systems occurs (Buldyrev, 2010).

5.1.5 Communication Efficiency Hypotheses Test

This section discusses the communication efficiency hypotheses tests. The table 4-4 presents the summary hypothesis test for the communication efficiency using the Mann-Whitney Test. For Hypothesis 3b, we can conclude that the median communication efficiency ($E(G)_L$) of the legacy maritime platform is significantly different from that of the future maritime platform at a 0.05 significance level, meaning that the maritime platform communication efficiency is higher than the legacy platform. For Hypothesis 4a2, we can conclude that the median communication efficiency ($E(G_{PGI})$) of the Italian power grid is significantly different from that of the legacy maritime platform at a 0.05 significance level, meaning that the legacy maritime platform' communication efficiency is reduced during random node failure. For Hypothesis 4b2, we can conclude that the median communication efficiency ($E(G_{PGI})$) of the Italian power grid is significantly

different from that of the future maritime platform at a 0.05 significance level, meaning that the Italian power grid communication efficiency is reduced during random node failure.

5.1.6 Data Validation

Finally, the Western and Italian power grid datasets were used for the model validation and baseline for comparison (see Appendix A). The two power grid interconnection datasets were obtained from previously published articles (Sole, 2007; Watts, 1998). The results of the degree-k distribution plots show an exponential distribution for the power grid. Table 5-1 shows the summary comparing published data with the experimental data results. The difference between the published data concerning nodes and links are shown in Table 5-1, Row 2 (Rosato, 2005; Sole, 2007) and the experimental data obtained from ENTSOE in (Row 3) was due to the 11-year expansion of the power grid system in Europe. The variations between the published value of the average degree-k (2.67) and the fragmentation threshold (0.63) were due to the formula used in the published data. In calculating the average degree-k, the published data use this formula $< k > = \frac{2L}{N}$ (Barabasi, 2016, Equation 2.2). In this research, however, we use the average (mean) formula < x > = (1/n)$\sum_{i=1}^{n} x_i$ (Barabasi, 2016; Box 2.2). We use the published data of both power grids to validate our model before proceeding with the simulations of the legacy and future shipboard data.

Table 5-1: Comparison of published data with experimental data results

Network	Nodes (N)	Links (L)	Average degree-k <k>	Shortest Path Length <l>	Fragmentation Threshold Fc	Average Closeness Centrality C_C	Network Efficiency E(G)
Italian Grid Published Data	272	368	2.70	8.47	.583	Note 1	.1181
Italian Grid Experiment	329	809	4.2	9.889	.30135	0.006602	.1200
Western Grid Published Data	4941	6594	2.67	Note1	.63	Note 1	Note1
Western Grid Experiment	3450	7153	2.07	1.204	.4861	Note 2	Note 2
legacy Platform Experiment	783	6716	8.59	5.375	.97968	0.007980	.1114
future Platform Experiment	920	8040	8.74	5.825	.96583	0.005778	.9777

Notes:

1. There is no published data.
2. Did not calculate the parameters since we use the Italian power grid data for comparison.

5.2 Conclusion

The goal of this research was to develop a percolation-based metric to quantify the resilience (robustness) and performance (efficiency) of the communication systems. This research successfully demonstrates the use of a percolation-based metric framework and provides a method of generating a rank-order resilience of system proposals. The percolation-based metric model is practical, can discriminate between alternative solutions, and can inform engineering decisions.

Despite the many definitions of resilience and the many quantitative measures in use, no consistent treatment of the resilience concept exists, and the utility of the quantitative metrics is domain-dependent. Although there are vast numbers of studies on resilience, none of the previous research has used the maritime system FIRD to measure a

communication system resilience and efficiency. Furthermore, most of the available software applications are domain specific, making it difficult to adapt and learn to use the software. The Gephi software was adopted in this study due to the ease required to learn and use it, its ability to compute datasets with more than 20,000 nodes, and its nature as open-source software.

We conclude from the percolation-based metric framework that percolation theory can quantify resilience (robustness) and efficiency, answering Hypotheses 1 through 4. Furthermore, a system's robustness must be balanced with its network efficiency. Rapid advances in computational intelligence, automation, and control systems have made systems more efficient but less robust to disruptive events. The future maritime platform has a smaller variance resulting from the fact that its nodes are clustered together, whereas the legacy maritime platform has a considerable variance resulting from nodes that are widely scattered. The design improvements in the future maritime platform design have resulted in a sparse network or minimal "clustered hubs" making it vulnerable to random disruptive events.

5.3 Contributions

This praxis adds to the body of knowledge concerning the quantification of communication systems by developing a percolation-based metric framework to measure system resilience (robustness) and performance (efficiency) when failure data is lacking. Through the combination of percolation theory and social network theory, a method of generating a rank order resilience and efficiency of system proposals is demonstrated. The combination of percolation and social network theory is applied in this context due to their ability to account for system dependencies and analyze systems with greater than

20,000 nodes, which current traditional methods cannot accomplish. This method is practical and straightforward, can distinguish between system proposals, and therefore can inform engineering decisions. Percolation theory and SNA were identified from the various literature concerning power grids, rail transport systems, and critical infrastructure. The following items are the significant contributions:

- A percolation-based metric framework was developed to model maritime platform communication system interdependencies. The maritime platform functional interface requirement documents (FIRD) were used to develop the node and link datasets required as input into the Gephi software.
- A robustness model was developed to compute the system-wide robustness (fragmentation threshold (f_c)) during the random failure of components and systems without relying on data concerning component and system failure.
- An efficiency model was developed to measure communication efficiency during the random failure of components and systems.
- The European Network of Transmission System Operator power grid map was used to model the Italian power grid. The power grid map is a real-time map that illustrates the comprehensive transmission system network in Europe.
- This praxis provides the first measurement of nodal distribution for the maritime platform.
- This praxis provides the first use of functional interface requirements documents to measure the maritime platform communication system's robustness and efficiency.

The framework presented in this praxis provides a rank order resilience measure of system proposals that can enable system designers to make informed decisions. The resilience (robustness) and communication efficiency values are normalized, meaning the value is between 0 and 1, to allow comparison of different communication systems.

5.4 Future Research

The model can be extended to develop other system parameters and identify system vulnerabilities. Some of the possible research areas are listed below.

- Development of an optimization model: This capability could identify weak nodes and network hubs, making it possible to optimize the network using rewiring techniques.
- Development of a cost model: A cost model can be designed and used to simulate future repair cost data by using the historical component repair cost data,
- Development of a fault tolerant model: Using the historical component repair mean time data, the system's fault tolerance can be predicted.
- Development of a rapidity model: Using historical mean-time-before-failure (MTBF) and mean-logistics-delay-time(MLDT) data, a rapidity measure can be quantified for use during system design.
- Development of a risk model: The failed components can be assigned a failure severity metric using the component importance measure.

References

Albert, R., Jeong, H., and Barabasi, A.L. (1999), "Diameter of the World-Wide Web," *Nature,* 401, 130-131.

Arora, S. (1998), The approximability of NP-hard problems, *ACM*, 337-348.

Ayyub, B.M. (2014), "Systems resilience for multi-hazard environments: definitions, metrics, and valuation for decision making," *Risk Analysis,* 34(2), 340-355, doi:10.1111/risa.12093

Bahun, K. A., Birregah, B., Chatelet, E., and Planchet, J-L. (2016), "A model to quantify the resilience of mass railway transportation system," *Reliability Engineering and System Safety,* 153, 1-14, doi:10.1016/j.ress.2016.03.015.

Barabasi, A-L., Albert, R. (1999), "Emergence of scaling in random networks," *Science*, 286, 509-512.

Barabasi, A-L., Albert, R., Jeong, H. (1999), "Mean-field theory for scale-free random network," *Physica A*, 272, 173-187.

Barabasi, A-L. (2016), *Network Science,* Cambridge University Press, Cambridge, pp. 20-270.

Barker, K., Ramirez-Marquez, J. E., Rocco, C. M. (2013), "Resilience-based network Component importance measure", Reliability Engineering and System Safety, 117, 89-87.

Benipayo, C. (2016), "Understanding system interdependence to improve the resilience of shipboard cyber-physical systems," *APCOSEC 2016 Conference* (pp. 1-25), Bangalore: APCOSEC.

Bhamra, R., Dani, S., and Burnard, K. (2011), "Resilience: the concept, a literature review, and future directions," *International Journal of Production Research,* 49(18), 5375-5393, doi:10.1080/00207543.2011.563826.

Bhatia, U., Kumar, D., Auroop, R., Ganguly, A.R. (2015), "Network science-based quantification of resilience demonstrated on the Indian railway network, "*PLOS One*, 1-17.

Blanchard, B.S. (2003), Logistics Engineering and Management (6th Edition), Pearson.

Boudali, H., and Dugan, J.B. (2005), "A discrete-time Bayesian network reliability modeling and analysis framework," *Reliability Engineering and System Safety,* 87(3), 337-349.

Broadbent, S.R., and Hammersley, J. M. (1957), "Percolation process: I. Crystals and mazes," *Proceedings of the Cambridge Philosophical Society*, 53, 629-641.

Broder, A., Kumar, R., Maghoul, F., Raghavan, P., Rajagopalan, S., Stata, R., Tomkins, A., and Wiener, J. (2000), "Graph structure in the web," *Computer Networks*, 33, 309-320.

Bruneau, M., Chang, S.E., Eguchi, R.T., Lee, G.C., O'Rourke, T.D., Reinhorn, A.M., Shinozuka, M., Tierney, K., Wallace, W.A., and von Winterfeldt, D. (2003), "A framework to quantitatively assess and enhance the science the seismic resilience of communities," *Earthquake Spectra,* 19(4), 733-752.

Buldyrev, S. V., Parshani, R., Paul, G., Stanley, E., and Havlin, S. (2010), "Catastrophic cascade failures in interdependent networks", *Nature,* 464, 1025-1028.

Busic, A., Vliegen, I., and Scheller-Wolf, A. (2012), "Comparing Markov Chains: Aggregation and precedence relations applied to sets of states, with applications to assemble-to-order systems," *Mathematics of Operational Research,* 37(2), 259-287.

Callaway, D.S., Newman, M. E .J, Strogatz, S.H., and Watts, D. J. (2000), "Network robustness and fragility: Percolation on random graph," *Physical Review Letters,* 85, 5468-5471.

Chang, S. E., and Shinozuka, M. (2004), "Measuring improvements in the disaster resilience of communities," *Earthquake Spectra,* 20(3), 739-755.

Chen, L., and Miller-Hooks, E. (2012), "Resilience: an indicator of recovery capability in intermodal freight transport," *Transportation Science,* 46(1), 109-123. doi:10.1287/trsc.1110.0376.

Chen, Z., Wu, J., Xia, Y., Zhang, L. (2018), "Robustness of interdependent power grids and communication networks: A complex network perspective," IEEE Transactions on Circuits and Systems, 65(1), 115-119.

Cohen, R., Erez, K., Ben-Avraham, D., and Havlin, S. (2000), "Resilience of the internet to random breakdown," *Physical Review Letters,* 85, 4626-4628.

Cohen, R., Havlin, S. (2003), "Scale-free networks are ultra-small," *Physical Review Letters,* 90, 058701.

Dabrowksi, C. and Mills, K (2006, March), "*A Program of Work for Understanding Emergent A Program of Work for Understanding Emergent Behavior in Global Grid System"* Retrieved from National Institute of Standards and Technology: https://www.nist.gov/sites/default/files/documents/itl/antd/NISTprogram.pdf

DAU (2018), *Defense Acquisition University*, https://www.dau.mil/, site accessed 2017-05-12.

Desale, D., *KD Nuggets*, https://www.kdnuggets.com/2015/06/top-30-social-network-analysis-visualization-tools.html, site accessed on 2018-08-18.

DHS. (2010), *Department of Homeland Security,* Retrieved from Department of Homeland Security: https://www.dhs.gov/, site accessed on 2017-07-16.

Dikbiyik, F., Tornatore, M., Mukherjee, B. (2014), "Minimizing the risk from disaster failures in optical backbone networks," *Journal of Lightwave Technology*, 32(18), 3175-3183.

Ellens, W. K. (2013), "Graph measures and network robustness," *AMS*, 1-12, https://arxiv.org/abs/1311.5064, site accessed on 2017-06-10.

Enjalbert, S., Vanderhaegen, F., Pichon, M., Ouedraogo, A., and Millot, P. (2011), "Assessment of transportation system resilience," *Human modeling in assisted transportation*, 335-341, doi:10.1007/978-88-470-1821-1_36

ENTSOE, *European Network of Transmission System Operators for Electricity*, https://www.entsoe.eu/map/Pages/default.aspx, site accessed 2017-10-11.

Erdos, P. and Renyi, A. (1959), "On random graphs," *Publicationes Mathematicae*, 6, 290-297.

Erdos, P. and Renyi, A. (1960), "On the evolution of random graphs," *Publications of the Mathematical Institute of Hungarian Academy of Sciences*, 5, 17-61.

Erdos, P. and Renyi, A. (1961), "On the strength of connectedness of a random graph," *Acta Mathematica Scientia Hungary*, 12, 261-267.

Ericson, C. I. (2016), *Hazard Analysis Techniques for System Safety*, Wiley, Hoboken, pp 430-432.

Estrada, E. (2003), *The Structure of Complex Networks, Theory, and Applications*, Oxford University Press, Oxford.

Faloutsos, M., Faloutsos, P., Faloutsos, C. (1999), "On power-law relationships of the internet topology," *Computer Communication Review*, 29, 251-262.

Filippini, R., Silva, A. (2012), "Resilience analysis of networked systems-of-systems based on structural and dynamic interdependence," *11th International Probabilistic Safety Assessment and Management Conference and the Annual European Safety and Reliability Conference 2012*, 5899-5905.

Franchin, P., and Cavalieri, F. (2015), "Probabilistic assessment of civil infrastructure resilience to earthquakes," *Computer-Aided Civil and Infrastructure Engineering*, 30(7), 583-600. doi:10.1111/mice.12092

Francis, R., and Bekera, B. (2014), "A metric and frameworks for resilience analysis of engineered and infrastructure systems," *Reliability Engineering and System Safety*, 121(01), 90-103.

Georger, S. R., Madni, A.M., and Eslinger, O.J. (2014), "Engineered resilient systems: A DoD perspective", *Conference on Systems Engineering Research* (pp. 1-8). Redondo Beach, CA.: Procedia Computer Science.

Gephi. (2017, November 11), *Gephi*, https://gephi.org, site accessed 2016-07-15.

Henley, E., Kumamoto, H. (1981), *Reliability Engineering and Risk Assessment*, Prentice-Hall, Inc., Englewood Cliffs, pp.40-44

Henry, D., and Ramirez-Marquez, J. E. (2012), "Generic metrics and quantitative approaches for system resilience as a function of time," *Reliability Engineering and System Safety*, 99(3), 114-122.

Hosseini, S., Barker, K., and Ramirez-Marquez, J.E. (2016), "A review of Definitions and Measures of System Resilience", *Reliability Engineering and System Safety*, 145(10), 47-61, doi:10.1016/j.ress.2015.08.006.

Huang, Z., Wang, C., Nayak, A., and Stojmenovic, I. (2015), "Small cluster in cyber-physical systems: Network topology, interdependence, and cascading failures," *IEEE Transactions on Parallel and Distributed Systems*, 26(8), 2340-2351.

Jackson, S. and Ferris, T. (2012), "Resilience principles for engineered systems," Systems Engineering, 16(2), 152-164.

Karrer, B., Newman, M.E.J., and Zdeborova, L. (2014), "Percolation of Sparse Network". Physical Review Letters, 113(208702), 1-6.

Khakzad, N., Khan, F., and Amyotte, P. (2013), "Risk-based design of process systems using discrete-time Bayesian networks," *Reliability Engineering and System Safety*, 109, 5-17, doi:10.1016/j.ress.2012.07.009.

Kutoglu, and T., Tumer, I.Y.. (2007), "FFIP: A framework for early assessment of functional failures in complex system," *International Conference on Engineering Design* (pp. 1-12). Paris: ICED.

Kurtoglu, T. and Tumer, I.Y. (2008), "A graph-based fault identification and propagation framework for functional design of complex system", *Journal of Mechanical Design,* 130(5), 1-8.

Kurtoglu, T., and Tumer, I.Y. (2010), "A functional failure reasoning methodology for evaluation of conceptual system architecture," *Research in Engineering Design*, 21(4), 209-234.

Latora, V. and Marchiori, M. (2001), "Efficient behavior of small-world networks," *Physical Review Letter,* 87(19), 1-4.

Latora, V. and Marchiori, M. (2003), "Economic small world behavior in weighted networks," *The European Physical Journal B-Condensed Matter and Complex System,* 32(2), 249-263.

Latora, V. and Marchiori, M. (2007), "A measure of centrality based on network efficiency," *New Journal of Physics*, 9(6), 1–11.

Lewis, E. (1994), *Introduction to Reliability Engineering,* John Wiley & Sons, Inc., Evanston, pp. 361-400.

Li, D., Zhang, Q., Zio, E., Havlin, S., and Kang, R. (2015), "Network reliability analysis based on percolation theory," *Reliability Engineering and System Safety*, 142(10), 556--562.

Lough, K. G., Stone, R., and Tumer, I.Y. (2009), "The risk in early design method," *Journal of Engineering Design,* 20(2), 155-173.

MAA (2018), https://www.maa.org/press/periodicals/convergence/leonard-eulers-solution-to-the-konigsberg-bridge-problem, site accessed 06-10-18.

Madni, A. and Jackson, S. (2009), "Towards a conceptual framework for resilience engineering", *IEEE Systems Journal*, 3(2), 181-191.

Mane, M., DeLaurentis, D., and Frazho, A. (2011), "A Markov perspective on development interdependencies in networks of systems," *Journal of Mechanical Design,* 133(10), 1-9.

Martins, L., Girao-Silva, R., Jorge, L., Gomes, A., Musumeci, F., Rak, J. (2017), "Interdependence between power grids and communication networks: A resilience perspective," *DRCN 2017 - Design of Reliable Communication Networks; 13th International Conference*, 154-162.

Mauthe, A., Hutchison, D., Cetinkaya, E.K., Ganchev, I., Rak, J., Sterbenz, J.P.G., Gunkel, M., Smith, P., Gomes, T. (2016), "Disaster-resilient communication networks: Principles and best practices, *Proceedings RNDM 2016, 8th International Workshop on Resilient Networks Design and Modeling*, 1-10.

Mehrpouyan, H., Haley, B., Dong, A., Tumer, I.Y., and Hoyle, C. (2013), "Resilient design of complex engineered systems against cascading failure," *Proceedings of the ASME 2013 International Mechanical Engineering Congress and Exposition* (IMECE2013-63308), 12, 1-11, doi:10.1115/IMECE2013-63308.

Mehrpouyan, H., Haley, B., Dong, A., Tumer, I.Y., and Hoyle, C (2015), "Resiliency analysis for complex engineered system design," *Artificial Intelligence for Engineering Design, Analysis and Manufacturing*, 29(1), 93-108, doi:10.1017/s0890060414000663.

Minitab. (2017), *Minitab 18*, www.minitab.com, site accessed 2017-11-01.

Molloy, M. and Reed, B. (1995), "A critical point for random graphs with a given degree Sequence," *Random Structures, and Algorithms*, 6, 161-179.

Nan, C., and Sansavini, G. (2016), "Building an integrated metric for quantifying the resilience of interdependent infrastructure system," *Critical Information Infrastructure Security*, 159-171.

NAVSEA. (2012), *SDM AND SIM MANUAL*, Washington, DC, US: Naval Sea Systems Command.

Newman, M., Barabasi, A-L., Watts, D. J. (2006), *The structure and dynamics of networks,* Princeton University Press, Princeton, pp. 167-408.

NIPP (2013), National Infrastructure Protection Plan, https://www.dhs.gov/national-infrastructure-protection-plan, site accessed 2017-06-15.

Omer, M., Mostashari, A., and Lindemann, U. (2014), "Resilience analysis of soft infrastructure systems," *Procedia Computer Science*, 28, 565-574. doi:10.1016/j.procs.2014.03.069

Ormon, S. W., Cassady, C.R., and Greenwood, A.G. (2002), "Reliability prediction models to support conceptual design," *IEEE Transactions on Reliability*, 51(2), 151-157.

Ouyang, M., and Duenas-Osorio, L (2012), "Time-dependent resilience assessment and improvement of urban infrastructure systems," *Chaos*, 22, 1-11.

Parandehgheibi, M., Modiano, E. (2013), "Robustness of interdependent networks: The case of communication networks and the power grid," *Globecon 2013 – Next Generation Networking Symposium*, 2164-2169.

Pool, I. De S., and Kochen, M. (1978), "Contacts and Influence," *Social Networks*, 1, 1-48.

Rad, Z.B., Jahromi, A.E. (2014), "A framework for resiliency assessment of power Communication networks," *Scientia Iranica E*, 21(6), 2399-2418.

Raghav, P., and Barker, K. (2012), "Building dynamic resilience estimation metrics for interdependent infrastructure," *Proceedings of the European Safety and Reliability Conference*, Helsinki, Finland, 624-632.

Rak, J., Hutchison, D., Calle, E., Gomes, T., Gunkel, M., Smith, P., Taplocai, J., Verbrugge, S., Wosinska, L. (2016), "RECODIS: Resilient communication services protecting end-user applications from disaster-based failures,"*Proceedings ICTON 2016 – 18th International Conference on Transparent Optical Networks*, 1-4.

Rinaldi, S.M., Peerenboom, J.P. and Kelly, T.K. (2001), "Identifying, understanding, and analyzing critical infrastructure interdependencies," *IEEE Control Systems Magazine*, 21(6), 11-25.

Rosas-Casals, M., Valverde, S., and Sole, R.V. (2007), "Topological vulnerability of the European power grid under errors and attacks," *International Journal of Bifurcation and Chaos*, 17(7), 2465-2475.

Rosato, V., Bologna, S., and Tiriticco, F. (2005), "Topological properties of high-voltage electrical transmission networks" *Electric Power Systems Research*, 77(2), 99-105.

Rose, A. (2007), "Economic resilience to natural and man-made disasters: multidisciplinary origins and contextual dimensions," *Environmental Hazard*, 7(4), 383-398.

Small, C., Parnell, G., Pohl, E., Goerger, E., Cottam, B., Specking, E., Wade, Z. ( ), "Engineered Resilient Systems with Value-Focused Thinking," *27th Annual INCOSE International Symposium*, 1-15.

Serrano, M.A., Krioukov, D., Boguna, M. (2008), Self-similarity of complex networks and hidden metric spaces, *Physical Review Letters*, 100(7), 1-4.

Sole, R. V., Rosas-Casals, M., Corominas-Murtra, B., and Valverde, S. (2007), "Robustness of the European power grids under intentional attack," Physical Review E, 77(2), 1-7.

Solomonoff, R. and Rapoport, A. (1951), "Connectivity of random nets," *Bulletin of Mathematical Biophysics*, 13, 107-117.

Song, Z., Ren, G., Mirabella, L., and Srivastava, S. (2016), "A resilience metric and its calculation for ship automation system," *2016 Resilience Week, IEEE*, 194-199.

Spiegel, M.R. (1994), *Theory and Problems of Statistics*, McGraw-Hill, New York.

Stone, R. B., Tumer, I. Y., and Van Wie, M. (2005), "The function-failure design method," *Journal of Mechanical Design*, 127(3), 397.

Sullivan, P. (2018), https://www.washingtonpost.com/national/as-hurricane-michael-recovery-begins-telecommunications-electrical-power-still-an-issue-in-florida-panhandle, site accessed 2018-10-20.

Traverse, J. and Milgram, S. (1969), "An experimental study of the small world problem," *Sociometry*, 32, 425-443.

Uday, P. and Marais, K. (2015), "Designing Resilient Systems-of-Systems: A Survey of Metrics, Methods, and Challenges," *Systems Engineering*, 18(5), 491-510.

Uusitalo, L. (2007), "Advantages and Challenges of Bayesian Networks in Environmental Modeling," *Ecological Model*, 312-318.

Vesely, W. G. (1981), *Fault Tree Handbook.* Washington, DC: Systems and Reliability Research, Office of Nuclear Regulatory Research, USNRC.

Wade, J. and Madni, A. (2011), "An Integrated, Modular Research Architecture for the Transformation of System Engineering," *CSER 2011* (p. 10). Los Angeles, CA: University of Southern California.

Wang, J., and Rong, L-L. (2009), "Cascade-based attack vulnerability on the US power grid," *Safety Science*, 47(10), 1332-1336.

Watts, D., and Strogatz, S. H. (1998), *cdg.columbia.edu*, http://cdg.columbia.edu/cdg/datasets, site accessed 2017-07-30.

Watts, D., and Strogatz, S. H. (1998), "Collective dynamics of small-world networks," *Nature*, 393, 440-442.

Wheaton, M. and Madni, A. (2015), "Resiliency and affordability attribute in a system integration trade space," *AIAA Space 2015 Conference and Exposition* (pp. 1-8). Pasadena: AIAA Space Forum.

Woods, D.D. (2015), "Four concepts for resilience and the implications for the future of resilience engineering," *Reliability Engineering and System Safety*, 141, 5-9.

Youn, B.D., Hu, C. and Wang, P. (2011), "Resilience-driven system design of complex engineered systems," *Journal of Mechanical Design*, 133(10), 1-15.

Zimmerman, A. (2018), Live Science, https://www.livescience.com/20718-computer-history.html, site accessed 2018-05-10.

Zobel, C. W. (2011), "Representing perceived tradeoffs in defining disaster resilience," *Decision Support System*, 50(2), 394-403.

Appendix A

Part A. Model Validation

Part A. Estimation of Difference for Italian Power grid

Sample 1: Italian grid results using Inverse Percolation

Sample 2: Italian grid published data

Two-Sample T-Test and CI

Method

μ_1: mean of Sample 1

μ_2: mean of Sample 2

Difference: $\mu_1 - \mu_2$, *Equal variances are not assumed for this analysis.*

Descriptive Statistics

Sample	N	Mean	StDev	SE Mean
Sample 1	329	4.20	3.27	0.18
Sample 2	272	2.70	3.03	0.18

Estimation for Difference

Difference	95% CI for Difference
1.497	(0.992, 2.002)

Test

Null hypothesis	$H_0: \mu_1 - \mu_2 = 0$
Alternative hypothesis	$H_1: \mu_1 - \mu_2 \neq 0$

T-Value	DF	P-Value
5.82	591	0.000

Difference	95% CI for Difference
1.497	(0.992, 2.002)

Part B. Estimation of Difference for Western Power grid

Sample 1: Western Power grid Inverse Percolation result

Sample 2: Western Power grid published data

μ_1: mean of Sample 1

μ_2: mean of Sample 2

Difference: $\mu_1 - \mu_2$, *Equal variances are not assumed for this analysis.*

Descriptive Statistics

Sample	N	Mean	StDev	SE Mean
Sample 1	3450	2.07	1.52	0.026
Sample 2	4941	2.67	2.77	0.039

Estimation for Difference

Difference	95% CI for Difference
-0.6000	(-0.6925, -0.5075)

Test

Null hypothesis $H_0: \mu_1 - \mu_2 = 0$

Alternative hypothesis $H_1: \mu_1 - \mu_2 \neq 0$

T-Value	DF	P-Value
-12.72	8002	0.000

Appendix B

Table Appendix B List of Domains with Resilience Research

Resilience Research Topic

Categories	**Journal Papers**	**%**
1. Ecology	3960	5.25%
2. Environmental Sciences	3928	5.20%
3. Engineering Electrical Electronics	3834	5.08%
5. Psychiatry	2997	3.97%
6. Environmental Studies	2798	3.71%
7. Telecommunications	2304	3.05%
8. Computer Science Methods	1993	2.64%
9. Computer Science Information Systems	1925	2.55%
10. Psychology, Multidisciplinary	1799	2.38%
11. Public Environmental Occupational Health	1793	2.37%
12. Water Resources	1455	1.93%
13. Psychology, Clinical	1417	1.88%
14. Marine Freshwater Biology	1403	1.86%
15. Neurosciences	1295	1.72%
16. Computer Science Hardware Architecture	1278	1.69%
17. Multidisciplinary Science	1277	1.69%
18. Psychology, Developmental	1176	1.56%

19. Geosciences, Multidisciplinary	1167	1.55%
20. Social Work	1098	1.45%
21. Geography	990	1.31%
22. Psychology	968	1.28%
23. Family Studies	910	1.21%
24. Computer Science Software Engineering	909	1.20%
25. Economics	908	1.20%
26. Engineering, Civil	901	1.19%
27. Education, Educational Research	869	1.15%
28. Bio-diversity Conservation	839	1.11%
29. Meteorology, Atmospheric Science	824	1.09%
30. Computer Science Artificial Intelligence	798	1.06%
31. Social Sciences, Interdisciplinary	783	1.04%
32. Management	748	0.99%
33. Gerontology	739	0.98%
34. Planning Development	727	0.96%
35. Nursing	689	0.91%
36. Forestry	685	0.91%
37. Sociology	649	0.86%
38. Plant Sciences	634	0.84%
39. Oceanography	625	0.83%
40. Clinical Neurology	580	0.77%

41. Urban Studies	577	0.76%
42. Psychology, Social	543	0.72%
43. Computer Science Interdisciplinary Apps	535	0.71%
44. Green Sustainable Science	534	0.71%
45. Optics	509	0.67%
46. Engineering, Environmental	507	0.67%
47. Psychology, Applied	495	0.66%
48. Geography, Physical	495	0.66%
49. Operational Research Mgmt. Science	486	0.64%
50. Political Science	485	0.64%
51. Pediatrics	479	0.63%
52. Imaging Science	473	0.63%
53. Biology	455	0.60%
54. Engineering, Industrial	438	0.58%
55. Polymer Science	421	0.56%
56. Materials Science, Interdisciplinary	421	0.56%
57. Fisheries	411	0.54%
58. Business	406	0.54%
59. International Relations	400	0.53%
60. Medicine, General Internal	392	0.52%
61. Soil Science	387	0.51%
62. Social Sciences, Biomed	387	0.51%

63. Rehab	382	0.51%
64. Behavioral Science	382	0.51%
65. Pharmacology, Pharmacy	362	0.48%
66. Biochemistry, Molecular Bio	362	0.48%
67. Psychology, Educational	360	0.48%
68. Geriatrics	360	0.48%
69. Energy	358	0.47%
70. Agriculture	350	0.46%
71. Health Care	347	0.46%
72. Anthropology	336	0.45%
73. Automation Controls	323	0.43%
74. Construction Building Technology	320	0.42%
75. Evolutionary Biology	316	0.42%
76. Food Science	313	0.41%
77. Health Policy	303	0.40%
78. Agronomy	294	0.39%
79. Physics Applied	271	0.36%
80. Oncology	265	0.35%
81. Public Admin	262	0.35%
82. Engineering, Multidisciplinary	260	0.34%
83. Genetics	259	0.34%
84. Microbiology	258	0.34%

85. Area Studies	256	0.34%
86. Engineering, Chemical	241	0.32%
87. Business, Finance	239	0.32%
88. Criminology	230	0.30%
89. Engineering, Mechanical	227	0.30%
90. Zoology	225	0.30%
91. Limnology	218	0.29%
92. Transportation Science	211	0.28%
93. Endocrinology	202	0.27%
94. Math Applied	201	0.27%
95. Biotech	201	0.27%
96. History	198	0.26%
97. Math Interdisciplinary	188	0.25%
98. Hospitality	188	0.25%
99. Social Issues	186	0.25%
100. Chemical Physical	172	0.23%
101. Engineering, Manufacturing	165	0.22%
Total	**75499**	**100.00%**